

1 **Rolling back the ‘mudstone blanket’: complex geometric and facies responses to basin architecture**
2 **in the epicontinental Oxford Clay Formation (Jurassic, UK)**

3 Mark A. Woods^{a*}, Jan A. I. Hennissen^a, Andrew J. Newell^b, Keith L. Duff^c, Philip R. Wilby^a

4 ^aBritish Geological Survey, Keyworth, Nottingham, UK, NG12 5GG

5 ^bBritish Geological Survey, Maclean Building, Wallingford, UK, OX10 8BB

6 ^c 21 Bishops Walk, Barnack, Stamford, Lincs, UK, PE9 3EE

7 *Corresponding author: Email: maw@bgs.ac.uk

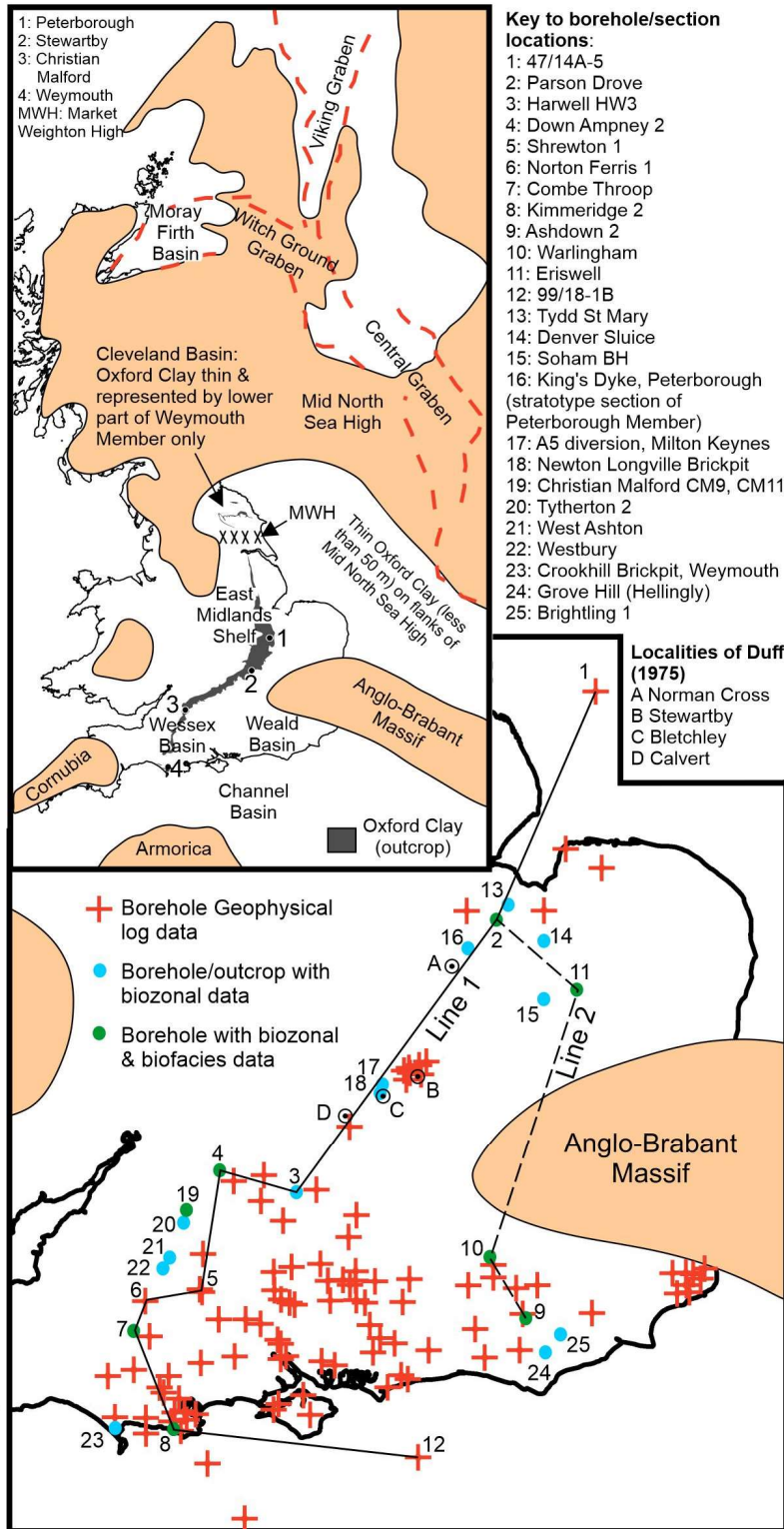
8 **Abstract**

9 Facies variability of mudstones is likely greater than generally perceived, with important implications
10 for their behaviour in major civil engineering, energy and waste disposal applications. Here, we
11 explore this variability for the UK Oxford Clay, a widely studied Middle/Upper Jurassic mudstone.
12 Evidence from wire-line logs, geochemistry, sequence stratigraphy and biofacies analyses are
13 combined to reveal heterogeneity within the Peterborough Member (Lower Oxford Clay) and to
14 explore the extent to which it blanketed basin features or responded dynamically to them. Thickness
15 modelling suggests that the Mid North Sea High, formed by Mid Jurassic thermal doming, likely
16 influenced sediment pathways, favouring thick sediment accumulation in the Wessex Basin, thinner
17 successions across the East Midlands Shelf, and sediment starvation in the Weald Basin. Biofacies
18 patterns, determined using a novel combination of detrended correspondence and cluster analysis,
19 vary significantly and suggest a complex patchwork of environments related to local basin setting.
20 The Type Section of the Peterborough Member seems to represent only a narrow range of
21 conditions that influenced its deposition, and cautions against developing basin-scale models based
22 on a few well exposed and heavily researched outcrop successions.

23 **Key Words:** Callovian, mudstone, heterogeneity, sequence stratigraphy, XRFs chemostratigraphy,
24 biofacies

25 **1. Introduction**

26
27 Recent research on the processes of mudstone deposition question the long-held view that these
28 sediments can be understood as a ‘mud-blanket’ resulting from slow deposition from suspension in
29 quiet water conditions (e.g. Scheiber et al. 2007, Macquaker and Bohacs 2007, Birgenheier et al.
30 2017). Earlier work on both the Oxford Clay (Hudson and Martill 1991) and the Kimmeridge Clay
31 (Wignall, 1989) suggested that more episodic depositional events, including storms, may be
32 important factors in mudstone accumulation. Temporal and spatial variability of facies in the lower
33 part of the Oxford Clay were mentioned by Hudson and Martill (1991), and wider evidence of
34 mudstone facies heterogeneity has emerged from outcrop and borehole studies (Macquaker 1994,
35 Macquaker and Howell 1999, Birgenheier et al. 2017). Here, we adopt a multidisciplinary surface-to-
36 subsurface approach to test the extent of facies variation at basin scale across a range of contrasting
37 palaeogeographical settings for part of the Oxford Clay Formation (Peterborough Member) – a mud-
38 dominated unit that has historically been regarded as generally uniform (Callomon 1968, Holloway
39 1985). Limited outcrop studies point to the presence of vertically stacked lithofacies that can be
40 related to patterns of relative sea level change and sequence stratigraphy frameworks (Partington et
41 al. 1993, Macquaker 1994, Norris and Hallam 1995, Macquaker and Howell 1999, Hesselbo 2008).
42 Our work combines these localised outcrop data with an extensive subsurface data archive,



43 **FIGURE 1**

44 providing a fully contextualised model-based understanding of the likely extent of facies variability
45 across the entire preserved basin, allowing understanding of the role of structural/bathymetric
46 features in controlling facies patterns.

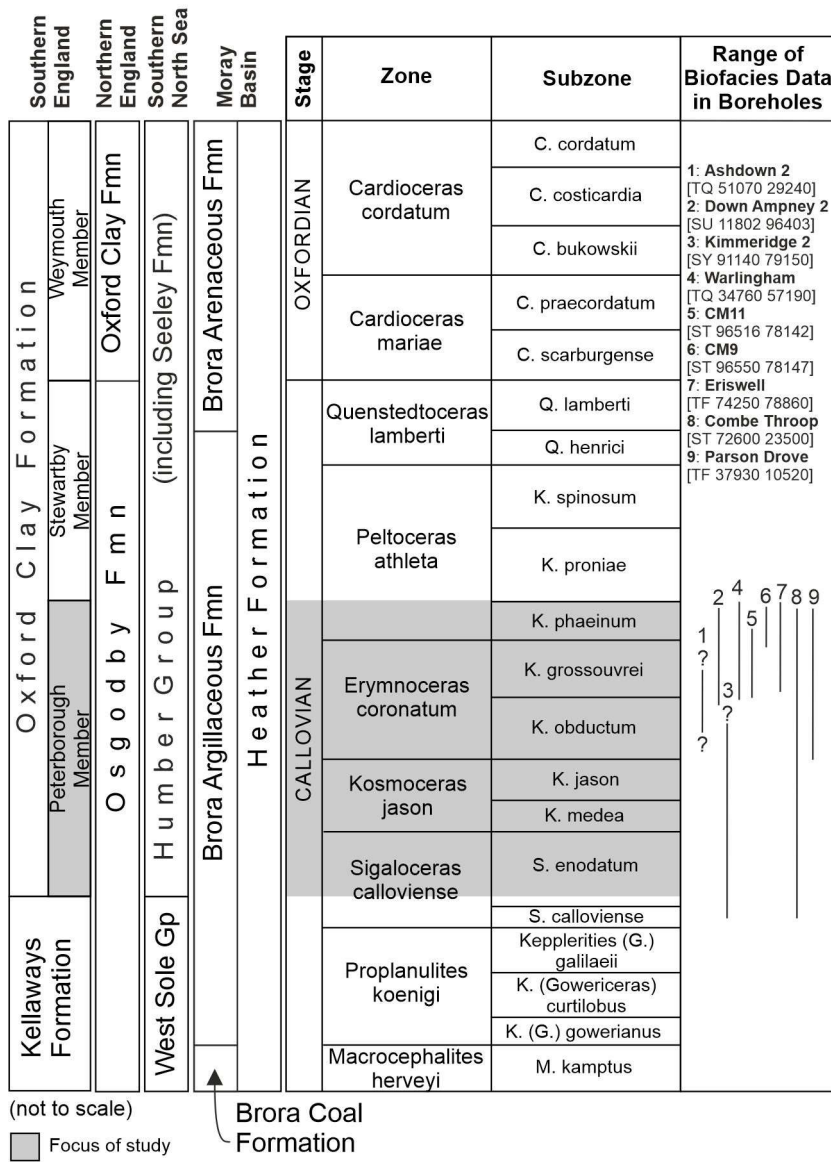
47 Current knowledge of the Oxford Clay is strongly influenced by a few well-exposed onshore
48 sites distributed across its outcrop (particularly the type sections of the component members in
49 Cambridgeshire (Peterborough Member), Bedfordshire (Stewartby Member) and Dorset (Weymouth
50 Member); e.g. Hudson and Martill 1991, 1994, Kenig et al. 1994, Macquaker and Howell 1999, Page
51 et al. 2009; Figs 1, 2). These outcrops, however, provide an incomplete picture of the Oxford Clay
52 because much of the formation is concealed beneath a thick (up to 1km) cover of younger strata in
53 areas such as the Wessex-Channel Basin in southern England. Fortunately, a long history of
54 hydrocarbons exploration in these deep basins has left a rich source of borehole information. Here,
55 we make use of this subsurface information to elucidate the extent of facies heterogeneity in the
56 lower part of the Oxford Clay (Peterborough Member) and its relationship to basin architecture. To
57 achieve this we: 1) use borehole geophysical logs and biostratigraphical data to understand patterns
58 of sediment thickness with respect to major palaeogeographical and basin structural features; 2)
59 combine new geochemical data with existing knowledge to refine understanding of the impact of
60 relative sea level change; and 3) explore variability in biofacies data for a series of distinct basin
61 settings (shallow platform, shallow shelf, shallow flooded massif, intra-basinal high, deep shelf,
62 faulted basin margin, distal basin) in order to resolve the extent to which environmental signals are
63 reflected in the gross lithological character of local successions.

64 Key objectives of this study are to: 1) understand basin-scale facies variability for the
65 Peterborough Member, and the extent to which it behaves as a 'mud blanket'; 2) develop
66 conceptual understanding of how basin architecture might influence sediment fluxes and
67 environments across the basin, and how these relate to facies variability; and 3) understand the
68 extent to which any heterogeneity in the Peterborough Member might be replicated in other
69 Jurassic mudstones. More broadly, our new digital model provides a resource for future assessment
70 of regional physical property variation in mudstones like the Oxford Clay, of particular relevance to
71 planned infrastructure development (National Infrastructure Commission 2018), and their suitability
72 as a host rock for nuclear waste storage (Delay et al. 2007, Butler 2010; Norris 2017).

73 **2. Geological Setting**

74 Deposition of the Oxford Clay Formation (Callovian/Oxfordian) coincided with a period of marked
75 crustal extension and fracturing associated with North Atlantic rifting (Wilhelm 2014). Mid Jurassic
76 (Late Toarcian – Bathonian) thermal doming of the North Sea region began to subside in the Early
77 Callovian (Underhill 1998), although the dome flanks persisted as a positive structural entity
78 (Bradshaw et al. 1992). These features added to a complex palaeogeographical fabric in the UK
79 region, where an epicontinental sea, dotted with emergent island massifs and cut by extensional
80 basins controlled by reactivated Variscan structures, formed the environment for deposition of the
81 Oxford Clay Formation (Fig. 1).

82 The Oxford Clay Formation is subdivided into three parts: the Peterborough, Stewartby and
83 Weymouth members (Fig. 2). The lowermost Peterborough Member is the most organic-rich part of
84 the formation, comprising brownish-grey mudstones and silty mudstones with typically 3 – 16 % TOC
85 (Kenig et al. 1994), plus occasional sandstone and concretionary limestone units. Compositionally, it
86 is a mixture of mica, illite, mixed illite/smectite, kaolinite and quartz, with calcite from shell beds,
87 foraminifera and nannofossils, and amorphous organic matter derived from marine phytoplankton
88 (Kenig et al. 1994; Macquaker 1994; Norry et al. 1994). The highest organic-rich mudstone unit
89 defines the top of the Peterborough Member. Younger parts of the formation (Stewartby and
90 Weymouth members; Fig. 2) typically comprise massive, paler grey silty mudstone (Cox et al. 1992)



91 FIGURE 2

92 and are less organic-rich, suggesting a more oxidizing depositional environment (Kenig et al. 1994). A
93 thin limestone interval (Lamberti Limestone) or equivalent shell bed/siltstone separates the
94 Stewartby and Weymouth members (Cox et al. 1992). In northern England (Yorkshire), deposition
95 was strongly influenced by a shallow structural block (Market Weighton High; Fig. 1) and the
96 Peterborough and Stewartby members are replaced by sandstones of the Osgodby Formation (Cope
97 2006, Powell et al. 2018, fig. 13; Fig. 2). This facies transition and thinning of the Oxford Clay across
98 eastern England into the Cleveland Basin was documented by Penn et al. (1986). Across the rest of
99 southern England, thickness data for the Peterborough Member indicate around 17 m at
100 Peterborough on the East Midlands Shelf (Hudson and Martill 1994), ca. 10.5 m in the Eriswell
101 Borehole (Bristow et al. 1989) on the flanks of the Anglo-Brabant Massif, ca. 15 – 18 m in boreholes
102 in the Weald Basin (Lake et al. 1987), and about 22 m near Weymouth on the Dorset coast
103 (Callomon and Cope 1995).

104 Offshore, strata equivalent to the Oxford Clay are sandy and silty in the Southern North Sea
105 (Seeley Formation; Lott and Knox 1994; Fig. 2), become deltaic and coal-bearing in the Central
106 Graben (Møller and Rasmussen 2003), and return to marine, mud and silt-dominated facies (Heather
107 Formation; Fig. 2) in the Moray Firth and Viking Graben (Underhill and Partington 1993). Across
108 southern England and the adjacent offshore regions the top of the Oxford Clay is widely conformable
109 with the overlying Corallian Group, except where the West Walton Formation has eroded into the
110 top of the Weymouth Member (Penn et al. 1986), or where the Corallian Group has been completely
111 removed by later erosion.

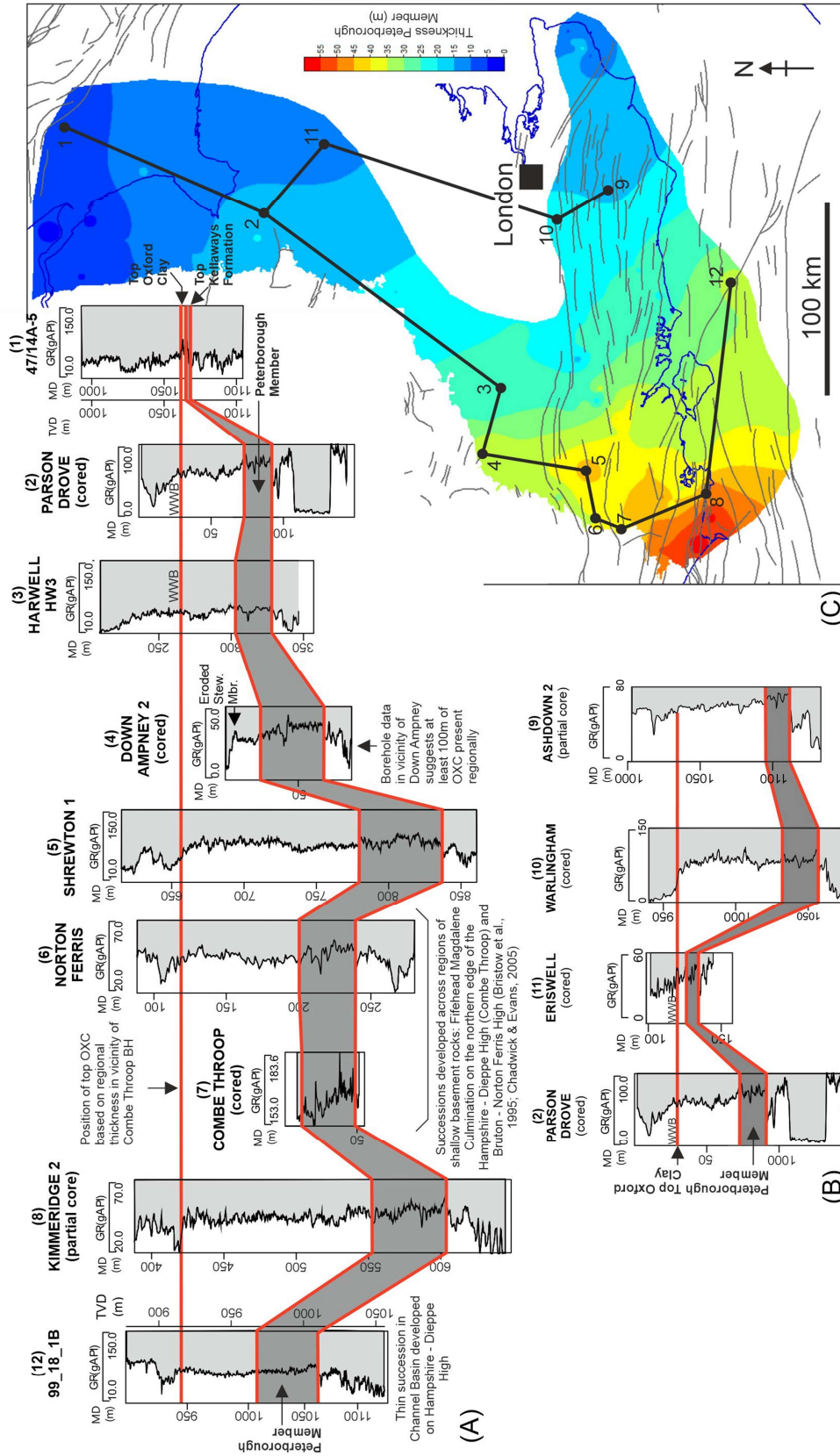
112

113 **3. Materials and Methodology**

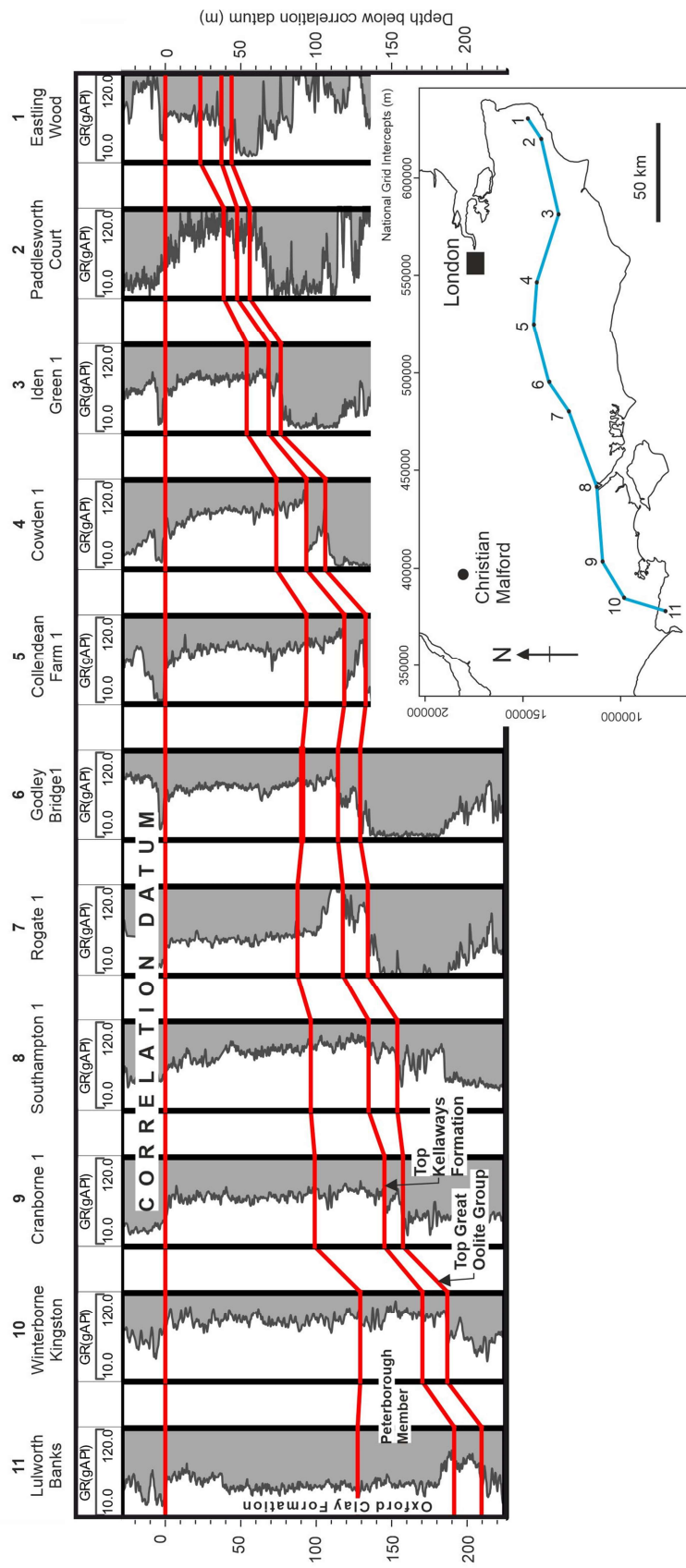
114 Determining the likely range and extent of basin-scale facies patterns in the Peterborough Member
115 requires broader knowledge of the depositional system that influenced those patterns. Key factors
116 are basin architecture, sea level fluctuation, and knowledge of environmental gradients (e.g.
117 oxygenation, wave energy) at different locations across the depositional landscape. To meet these
118 requirements our multidisciplinary approach uses borehole geophysical, lithological and biozonal
119 data to understand stratigraphical patterns and model sediment geometry; geochemistry to
120 interpret sea level fluctuation and its impact on the length of sediment pathways; and biofacies data
121 to infer environmental signals across contrasting basin settings. The large archive of subsurface data
122 (borehole core, geophysics, biostratigraphy) for the Peterborough Member held by the British
123 Geological Survey (BGS) provides both the spatial extent and stratigraphical resolution required by
124 the scale of this study.

125 **3.1 Regional geophysical log interpretation**

126 The inflection patterns of borehole geophysical logs in the Oxford Clay are usually sufficiently
127 distinctive to allow recognition of its component formations (Whittaker et al. 1985, Penn et al.
128 1986), with the elevated organic content of the Peterborough Member typically corresponding with
129 a higher gamma log response. Stratigraphic picks for the Oxford Clay were made mostly from gamma
130 ray and sonic logs for ca. 127 boreholes across southern, central and eastern England and adjacent
131 areas of the Channel and Southern North Sea basins (Figs 1, 3 and 4). Where present, stratigraphical
132 picks were made for the top of the Great Oolite Group (Cornbrash Formation), Kellaways Formation,
133 Peterborough Member, Stewartby Member and Weymouth Member, as well as associated
134 unconformities and faulted contacts. An important first step in this process was calibrating log
135 responses against known Oxford Clay stratigraphy in boreholes that, in addition to a suite of
136 geophysical logs, had associated core (Callomon and Cope 1971, Whittaker et al. 1985, Penn et al.
137 1986, Bristow et al. 1989, 1995 fig. 36) and biostratigraphical data (Gallois 1979, Cox 1977, 1984,



138 FIGURE 3



139 **FIGURE 4**

140 1988, 1991, Gallois and Worssam 1983, Buckley et al. 1991). These reference boreholes provided an
141 important constraint on extending stratigraphical interpretations into boreholes where only
142 geophysical logs and cuttings information were available. Interpretations were checked for internal
143 consistency using a grid of intersecting borehole correlation panels, and by flattening correlations on
144 multiple horizons to explore stratigraphical and structural trends.

145 Stratigraphic picks were subsequently used to create a refined thickness model of the
146 Peterborough Member and wider Oxford Clay Formation. Maps were interpolated using Discrete
147 Smooth Interpolation (DSI) (Mallet 1989) in SKUA-GOCAD™ software from borehole thickness data
148 that was corrected for both deviated borehole paths and variable structural dip.

149 **3.2 Lithological data**

150 Lithological information is provided by pre-existing boreholes in BGS archives, supplemented by two
151 newly drilled boreholes near Christian Malford, Wiltshire (Fig. 1), as well as information collated
152 from published records, BGS technical reports and unpublished borehole logs in BGS data archives.
153 The boreholes at Christian Malford are continuously cored and provide an important record of the
154 succession across the Coronatum/Athleta Zone boundary (Fig. 2) in an area where data are sparse.
155 Pre-existing borehole data (boreholes 2, 4, 9 – 11 of Fig. 2) relate to historical BGS work on the
156 Oxford Clay, and are represented by discontinuous core samples. These boreholes were selected
157 from the BGS archive to optimise core sample density (typically 0.1 m or less) and provide
158 representative stratigraphical and geographical coverage of the Peterborough Member. Lithological
159 descriptions of discontinuous core samples were made using a binocular microscope during
160 acquisition of biofacies data for these successions (see 3.4 below), and the observations used to
161 construct synthetic graphical borehole logs, supplemented by information from pre-existing logs and
162 reports where available and relevant.

163 **3.3 Geochemistry**

164 A newly drilled cored borehole (CM11; Fig. 1) in the higher part of the Peterborough Member
165 (Coronatum & Athleta biozones; Fig. 2) at Christian Malford, Wiltshire, provided material for
166 geochemical analysis (Fig. 5). Borehole CM9, drilled as part of a previous investigation at Christian
167 Malford (Hart et al. 2016, 2019) and partially overlapping with CM11, provided material for analysis
168 in the higher part of the Phaeinum Subzone.

169 Geochemical data were obtained from slabbed core lengths of CM11 using a portable Niton
170 XLt 793 X-Ray Fluorescence Spectrometer (XRFS), fitted with a 40kV Ag anode X-ray tube and using
171 the 'Standard Soil Mode'. Measurements were made at 10 mm intervals and for 30 seconds along
172 the core length, with values checked for internal consistency against a designated standard
173 reference sample. This procedure was repeated for the partially overlapping succession in CM9 using
174 selected milled samples of core material, analysing for 120 seconds with the XRFS in a static semi-
175 automated configuration.

176

177 **3.4 Biofacies & biozonal data**

178 Biofacies data (Figs 5 – 9) characterise stratigraphical intervals according to the types and
179 abundances of fossil material, and use understanding of palaeoecological affinities of facies
180 components to infer environmental signals. The technique can reveal patterns of environmental
181 change that can be compared with variability in the lithological character of host sedimentary
182 successions. Previous work on the Peterborough Member (Duff 1974, 1975) has used biofacies from
183 outcrop data for a limited part of the depositional basin to understand stratigraphical shifts in
184 depositional conditions. This work expands application of these data to a network of sites across the

185 wider depositional basin in southern and eastern England, selected to capture responses in a
186 probable diverse range of environmental settings in contrasting palaeogeographical and structural
187 settings. We analyse the distribution of biofacies components in borehole core using
188 correspondence analysis and clustering to explore their relationships and patterns in their
189 stratigraphical distribution.

190 Biofacies data for the Peterborough Member, comprising more than 2200 observations of
191 core samples, were compiled for the following 8 cored borehole sites (Fig. 1): Christian Malford CM9
192 and CM11 (distal shallow marine shelf), Down Ampney 2 (proximal shallow marine shelf), Combe
193 Throop (intra-basinal high), Kimmeridge 2 (deep marine shelf), Warlingham (faulted epicontinental
194 basin margin), Ashdown 2 (distal marine epicontinental basin), Parson Drove (shallow marine
195 platform), and Eriswell (shallow flooded massif margin).

196 For the Christian Malford (CM11) Borehole, biofacies data were collected from half-core
197 samples (10 cm diameter) at 10 mm intervals, examining part and counter-part bedding surfaces.
198 Biofacies components (Appendix 1) assessed as part of this study cover a range of taxonomic
199 groupings, mostly genera but including some broader categories (e.g. ammonites, foraminifera)
200 where appropriate, and also include the occurrence of features like wood and coprolite. Relative
201 frequency of key biofacies components (Appendix 1) was assessed using a semi-quantitative scale,
202 based on threshold counts (present; common, 2 – 4 specimens; abundant, ≥ 5 specimens; plaster,
203 with numerous specimens covering core surface). Biofacies data for the other boreholes rely on
204 discontinuous core samples, for which observations of all surfaces of each sample are combined into
205 a single record with a modified assessment of relative frequency (present; few, 2 specimens;
206 common, ≥ 3 specimens). Biofacies data for the Peterborough Member, collected at sites in eastern
207 and central England (Duff 1974, 1975) and re-analysed as part of this work, are fully quantitative
208 observations of aerially extensive bedding planes.

209 Statistical analysis of biofacies data uses a combination of Detrended Correspondence
210 Analysis (DCA) and clustering (hierarchical clustering & Non-Euclidian Relational Clustering (NERC))
211 to explore: 1) the faunal composition of different samples; and 2) the grouping of samples into
212 coherent biofacies. NERC clustering is typically more suited to analysis of palaeontological data
213 which are incomplete (Vavrek 2016). However, because our data are from borehole core, with an
214 implied age/depth relationship between consecutive samples, we combine both hierarchical and
215 NERC clustering techniques in our results.

216 Primary data were conditioned by: removal of rare/ambiguous components that might
217 otherwise distort the analysis; merging records of related components (e.g. species within a genus);
218 coding sample composition, sample size and biozonal assignment, and standardising scale of relative
219 frequency (see *Supplementary Data* for detailed procedure). All statistical analyses were performed
220 in the open source environment R (R Core Team 2020) using the following packages: vegan (Oksanen
221 et al. 2018) (DCA analysis based on upper quartile biofacies components); NbClust (Charrad et al.
222 2014) (optimum number of clusters for each borehole based on analysis of primary data); rioja
223 (Juggins 2017) (hierarchical clustering); ecodist (Goslee and Urban 2007) (calculation of ecological
224 distance matrix); fossil (Vavrek 2016) (NERC cluster analysis). An ecological distance matrix is
225 required for NERC clustering, and for our semi-quantitative data we adopt the Sørensen dissimilarity
226 index (or Dice index), one of the most commonly used and effective presence/absence dissimilarity
227 measures (Southwood and Henderson 2000, Magurran 2004). Compilations of biofacies data for the
228 analysed boreholes and details of their statistical analysis are provided as *Supplementary Data*.

229 The boreholes that are the source of our biofacies data are part of a larger suite of cored
230 boreholes in the Peterborough Member across southern Britain, drilled in connection with BGS
231 regional mapping programmes that date back to the late 1960s. Biostratigraphical interpretations of
232 many of these successions, published in BGS memoirs and technical reports, were compiled for this

233 study to provide precise stratigraphical understanding of geophysical log signatures, to allow
234 accurate comparisons of biofacies data, and to provide additional insight into patterns of thickness
235 variation.

236 **Supplementary material:** Geophysical log correlations, geochemical data and detailed biofacies
237 data, methodology and results are available as *Supplementary Data*.

238 **4. Results**

239 Geophysical log data provide a highly resolved picture of thickness variation for the Peterborough
240 Member across Southern Britain, with correlation panels and biostratigraphical data compilation
241 emphasising regions that were the long-term focus of sedimentation and others where deposition
242 was persistently restricted (Figs 3, 4; 10). Cyclical trends in sedimentary geochemical data at
243 Christian Malford (Fig. 5) show a strong relationship with patterns of sedimentation and biofacies in
244 borehole core. Across the basin, biofacies data show significant lateral contrasts between sites (Fig.
245 6). The results for each category of data are discussed in turn below. Detailed compilations of our
246 results are provided as *Supplementary Data*.

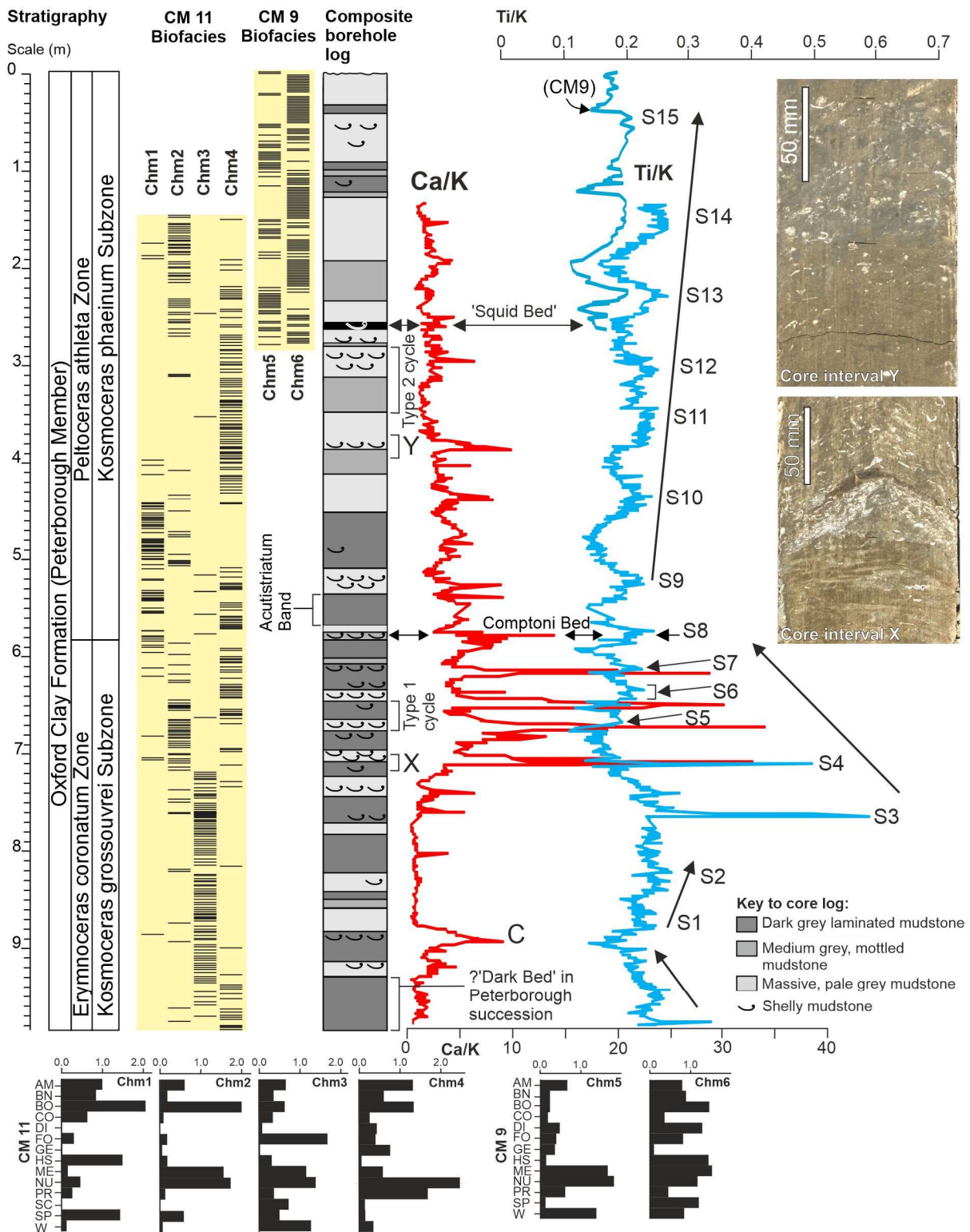
247 **4.1 Geophysical log correlation and basin modelling**

248 Along the northern margin of the Anglo-Brabant Massif (ABM), from the East Midlands Shelf in the
249 NE, towards the Wessex Basin in the SW, there is a consistent regional trend of thickening, for both
250 the Peterborough Member (<5 m to >55 m) and Oxford Clay Formation as a whole (<10 m to ca. 180
251 m) (Figs 3, 4). Significant thinning of the Peterborough Member (to ≤ 10 m) occurs on the flanks of
252 the ABM, and likely also the whole of the Oxford Clay, although erosion of the succession prevents
253 confirmation. The succession remains thin into the Weald Basin to the south, where the total Oxford
254 Clay Formation is about 80 m thick in the Ashdown 2 Borehole, with ca. 15 m representing the
255 Peterborough Member (Fig. 3). Offshore thickness trends are consistent with the onshore data, with
256 extremely thin (possibly incomplete) Oxford Clay inferred to occur in the southern North Sea (where
257 the formation is generally not separated from the parent Humber Group), and relatively thick
258 Peterborough Member (ca. 42 m) forming part of an eroded Oxford Clay succession in the Channel
259 Basin. As well as basin-scale features (e.g. ABM), there is an apparent association of local thickness
260 patterns with 1:1500000 -scale structural lineament data (Fig. 3A), seen in parts of the Wessex Basin,
261 for example local thickening near Shrewton, and thinning across the fault-bounded Norton Ferris
262 High (Chadwick and Evans 2005, figs 86, 88).

263 **4.2 Lithology**

264 Borehole CM11 proved a strongly cyclical succession of lithofacies that can be matched with
265 geochemical data (4.3 below; Fig. 5). Three broad lithofacies are recognised in borehole core: 1) pale
266 grey silty mudstone with abundant shell remains, dominated by nuculacean bivalves, including
267 specimens with articulated valves; 2) massive or very weakly fissile, medium – grey-brown silty
268 mudstone with scattered or sparse shell remains, but including occasional bedding-plane plasters of
269 the bivalves *Meleagrinnella* and/or *Bositra* and, 3) dark grey-brown, organic-rich laminated mudstone
270 with abundant plasters of *Bositra* and/or *Meleagrinnella*. The bases of shell beds may be sharply
271 defined or gradational, and cycles comprise either: 1) sharp-based shell bed with thin gradational
272 intervals of weakly fissile mudstone into dark laminated mudstone (Type 1; Fig. 5), or 2) weakly
273 fissile mudstone, with thicker gradational transition into a shell bed (Type 2; Fig. 5). Type 1 cycles are
274 thin (ca. 30 cm) and occur in the middle part of the borehole succession, and Type 2 cycles are
275 thicker (ca. 70 cm) and occur particularly in the higher parts of CM 11 (Fig. 5).

276



278 For sites across the rest of southern England, lithological data summarised on synthetic
279 borehole logs (Fig. 6) show that in the Wessex Basin, conspicuously silty mudstone dominates in the
280 lowest part of the Peterborough Member (Calloviense and Jason Zones) in the Kimmeridge 2 and
281 Combe Throop boreholes. In the Kimmeridge Borehole this diminishes with the appearance of dark
282 grey mudstone in the Coronatum Zone, but remains a persistent feature of the Combe Throop
283 succession. Bioclastic mudstone is a feature of the Coronatum Zone in the CM 9 and CM11
284 boreholes, and extends north-eastwards, in both the Down Ampney 2 and Parson's Drove
285 successions. In the Phaeinum Subzone, the rhythmic mudstone in CM9 and CM11 cannot be traced
286 into the Down Ampney 2 succession. Here, this interval contains a sharp contrast between darker
287 grey mudstone in the lower part of the subzone and much paler grey, biotubated mudstone in the
288 upper part. This change occurs immediately above a ca. 2.5 m thick laminated interval in the lower
289 part of the Phaeinum Subzone, that contains few fossils apart from wood, foraminifera and bone (Fig
290 6), and is unique to this borehole succession. A similar colour change occurs near the top of the
291 Peterborough Member in the Parson Drove succession on the East Midlands Shelf, although here the
292 lithology is laminated and silty, with greater development of dark mudstone in the underlying
293 Phaeinum Subzone. On the flanks of the ABM, the Coronatum Zone and Phaeinum Subzone in the
294 Eriswell Borehole comprises thin units of distinctively pale and medium grey, bioturbated mudstone
295 with abundant finely comminuted shell. The correlative interval thickens at the edge of the Weald
296 Basin in the Warlingham Borehole, where the lithology is rather uniformly bioclastic mudstone with
297 occasional laminated intervals, becoming distinctly silty in the upper part. The sparse data for the
298 central Weald Basin, from the Ashdown 2 Borehole, suggest a very different pattern of
299 sedimentation, with samples from the ?Coronatum Subzone represented by very dark brownish-
300 grey, hard, silty, pyritic calcareous mudstone.

301

302 **4.3 Geochemistry**

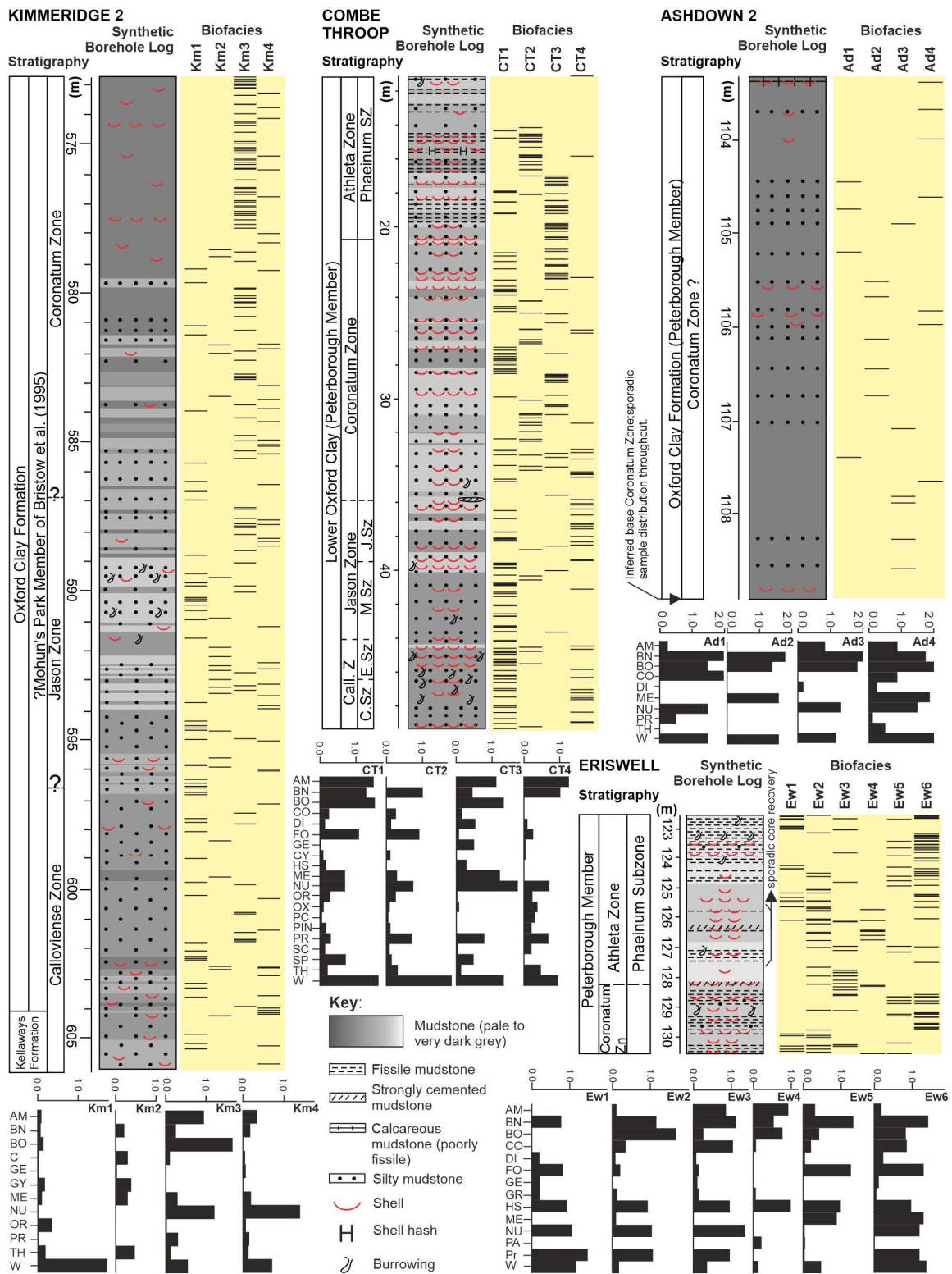
303

304 Titanium in the Peterborough Member shows a strong correlation with silica (Norry et al. 1994), and
305 functions as a proxy for variability in the flux of hydrodynamically heavy detrital components to the
306 depositional basin and/or winnowing. Figure 5 plots the variability of Ti normalised to K (the optimal
307 proxy for understanding detrital fluxes in the absence of XRF values for Si, Zr and Al) through the
308 CM11 and CM9 successions. The plot shows a strongly cyclic pattern, with an overall shift from
309 relatively high values in the lower 2.5 m of the succession (Coronatum Zone), to relatively lower
310 values in the middle part (interval above S4 and below S10 of Fig. 5), spanning the latest Coronatum
311 and earliest Athleta zones. Shell concentrations are picked out by the Ca/K plot, with those
312 characterising the Type 1 cycles in the CM11 succession forming four strong, closely spaced peaks
313 (S4 – S7; Fig. 5). An inflection in the trend of Ti/K data, from sharply falling to gradually increasing, is
314 coincident with the interval between two regionally extensive marker-beds in the Oxford Clay, the
315 Comptoni Bed and the overlying Acutistriatum Band (Hudson and Martill 1994; Fig. 5). Above these,
316 peaks S9 – S15 define a stacked succession of Type 2 cycles, with progressively increasing detrital
317 content and shell beds coincident with sharp peaks in the Ca/K curve.

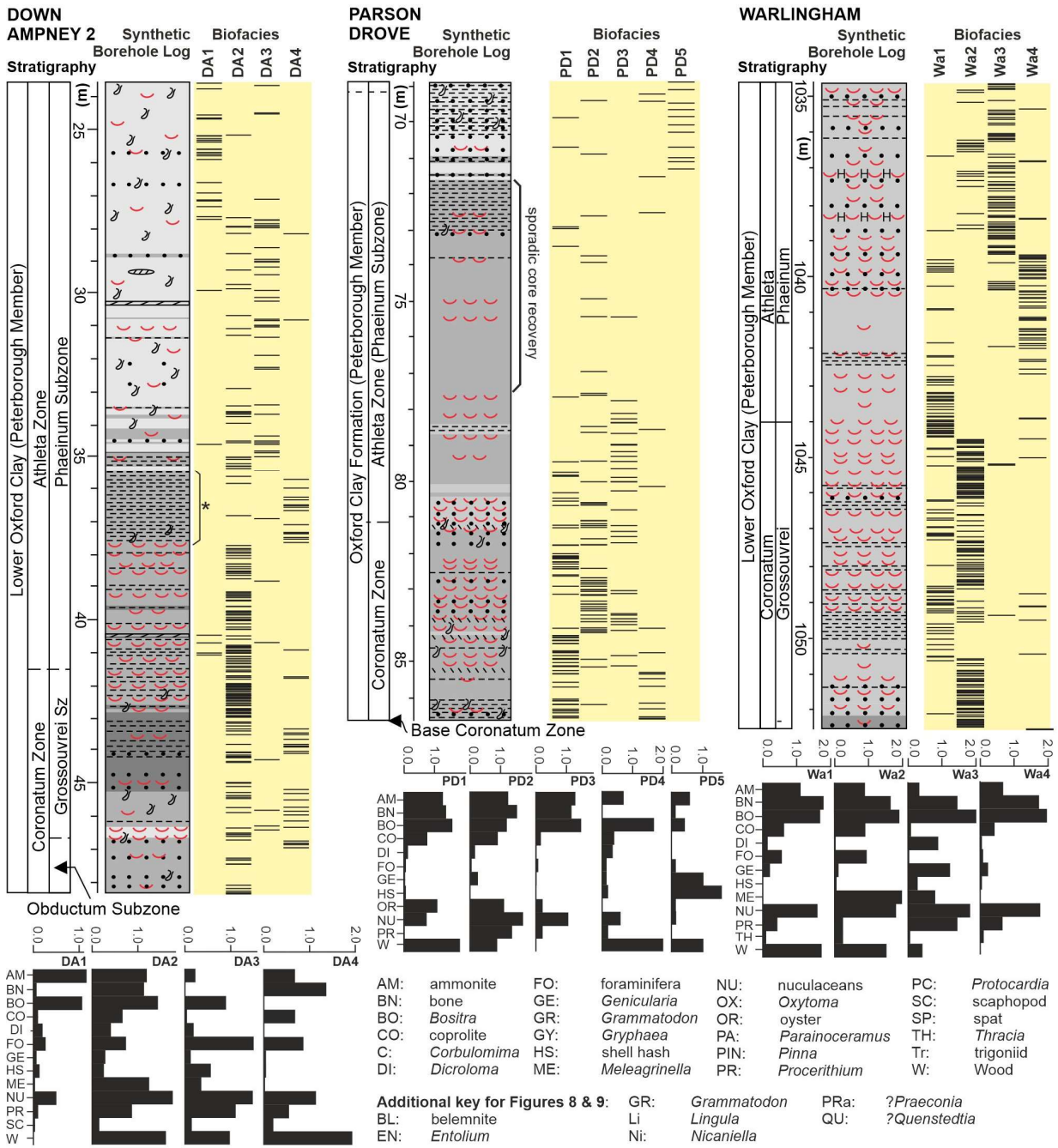
318

319 **4.4 Biofacies**

320 Litho- and biofacies variation occurs on a very fine (lamina) scale in the Oxford Clay (Macquaker and
321 Howell 1999). Our biofacies data resolves this fine-scale variation into decimetre-scale trends,
322 represented by the stratigraphical distribution of biofacies clusters (Figs 5 – 9), with the composition
323 of each cluster summarised as relative proportions in bar charts below each borehole log. The
324 number and composition of clusters is distinct for each site and determined by the data available for



325 FIGURE 6



326 FIGURE 6 (continued)

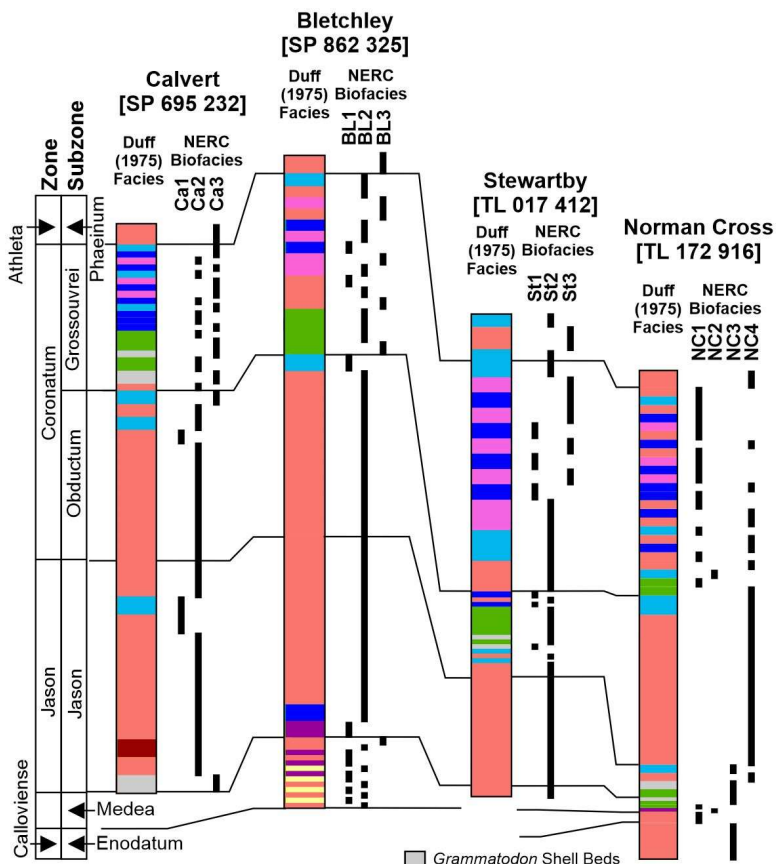
327 each site. Attempts to develop a unified biofacies classification across all sites forced removal of
328 components that were defining and common at individual sites, suggesting a significant degree of
329 site-specific biofacies character. Consequently, stratigraphical analysis of our biofacies data focuses
330 on identifying major contrasts in the arrangement and composition of biofacies within borehole
331 successions, and examining the extent to which these correspond with analogous or strongly
332 contrasting biofacies in correlative successions at other sites across the basin.

333 DCA plots of samples and taxa provide insight into which taxa are important for
334 characterising samples. DCA analysis for CM11 (Fig. 8A) is consistent with observations made during
335 borehole logging, and indicate two strongly contrasting end-members: 1) dark, organic-rich, fissile
336 mudstone dominated by remains of the thin-shelled bivalve *Bositra* (with or without *Meleagrinnella*);
337 2) Shell beds associated with pale grey mudstone with abundant thick-shelled nuculacean bivalves,
338 often associated with the gastropod *Procerithium* and sometimes also the serpulid *Genicularia*.
339 Most biofacies clusters comprise mixtures of these end member components, and are therefore
340 environmental composites that reflect the extent to which particular environmental settings are
341 more or less dominant at the scale of individual laminations.

342 Differences between biofacies cluster composition for a given borehole can be subtle or very
343 significant. Both the Warlingham and Parson Drove boreholes show a strong pattern of
344 stratigraphical specificity in the distribution of biofacies clusters, but several of the cluster
345 compositions are very similar, suggesting either a limited range of environmental change at these
346 sites, or smearing of the ecological signal by external factors. It is notable that the extremely shell-
347 rich Warlingham succession is characterised by an incongruent mixture of biofacies components
348 (e.g. *Bositra*, *Meleagrinnella*, nuculacean bivalves, *Genicularia*; Fig. 6) that characterise discrete
349 intervals elsewhere.

350 The successions in the Kimmeridge 2 and Combe Throop boreholes show a regular repetition
351 of biofacies clusters, with a tendency for particular biofacies to be slightly more dominant at some
352 levels (Fig. 6). Kimmeridge 2 also shows a pronounced stratigraphical and compositional shift in
353 biofacies at the top of the core log. In the Down Ampney 2 succession there is more marked
354 domination of particular intervals by particular biofacies clusters (Fig. 6), and these are also more
355 compositionally distinct, a pattern that is even more pronounced in the CM11 succession. The
356 largest number of biofacies clusters are associated with the highly condensed Peterborough
357 Member section at Eriswell (Fig. 6). Despite this, there is a strong unifying compositional feature (a
358 high proportion of shell hash and relative paucity of ammonites) that is unique to this site. Data for
359 Ashdown 2 are limited, but are notable for the extremely high proportions of bone and the bivalve
360 *Bositra* in all biofacies clusters.

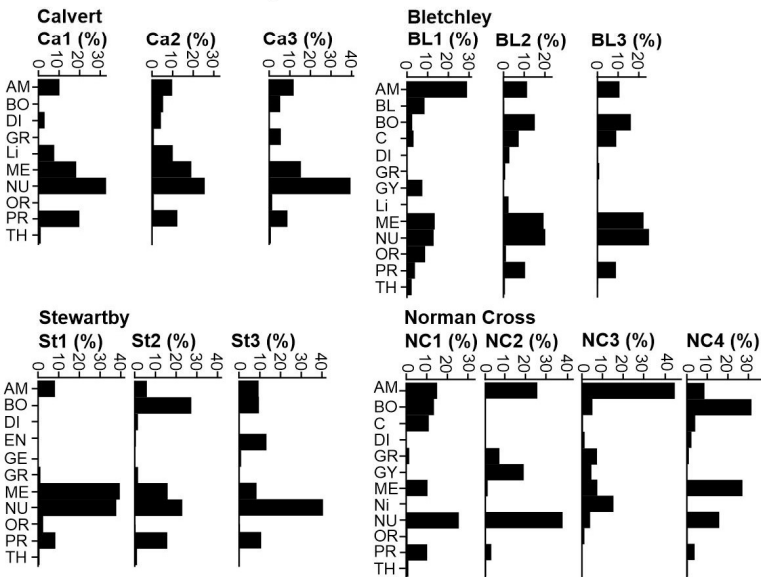
361 To explore the fidelity of our biofacies methodology and provide additional
362 palaeoenvironmental data, we have used the raw quantitative data collected by Duff (1975) as part
363 of his biofacies interpretation of the Peterborough Member (at Norman Cross near Peterborough,
364 Stewartby, Bletchley and Calvert) to generate biofacies classifications based on NERC clustering.
365 Figure 7 shows the correlation of the sections and compares the biofacies assignments of Duff
366 (1975) with those assigned using NERC. Both facies classifications show striking similarity in the
367 broad pattern of biofacies subdivisions for different biozonal intervals. The youngest and oldest
368 parts of successions show significant facies variability in both interpretations, with less variation in
369 the intervening part (Jason & Obductum subzones). In some cases there is direct correspondence of
370 biofacies recognised by Duff (1975) with biofacies clusters defined by NERC, and in other cases the
371 NERC analysis appears to be detecting contrasts identified by Duff (1975) although the boundaries of
372 these units are not necessarily coincident. These patterns, and the similarity in the taxa that define
373 distinct nodes in the DCA sample distribution (e.g. *Bositra*, *Meleagrinnella*, nuculaceans, oysters; Fig.
374



Key to biofacies of Duff (1975)

- █ Deposit Feeder Bituminous Shales
 - █ Nuculacean Shell Beds
 - █ Meleagrinnella Shell Beds
 - █ Calcareous Clays
 - █ Grammatodon-rich Bituminous Shales
 - █ Grammatodon Shell Beds
 - █ Gryphaea Shell Beds
 - █ Sands and Silty Clays
 - █ Blocky Claystone
- Vertical scale
1m

NERC Biofacies Cluster Composition



375 **FIGURE 7**

376 9) to other localities examined as part of this study (Fig. 8), suggests our combined NERC – DCA
377 methodology is robust in identifying meaningful environmental gradients.

378 NERC biofacies data for the localities described by Duff (1975) show that, generally, the
379 oldest parts of the succession (Enodatum/Medea subzones) seen at Norman Cross and Bletchley are
380 relatively rich in ammonites and oysters, but including at Norman Cross thin intervals with sharply
381 contrasting facies, where these faunal elements are sparse and *Bositra* more dominant. Higher in the
382 succession (Jason/Obductum subzones), facies at most localities are dominated by a mixture of
383 *Bositra*, *Meleagrinnella* and nukulacean bivalves, with the Obductum Subzone at Norman Cross and
384 Stewartby having a relatively higher proportion of *Bositra* compared to the corresponding interval at
385 Calvert. The distinctly more cyclic facies of the Grossouvrei Subzone contains frequent shell beds in
386 the Duff (1975) facies classification, corresponding with NERC facies clusters in which *Meleagrinnella*
387 and/or nukulacean bivalves tend to be more dominant compared to *Bositra*. The appearance of
388 more shell-dominated facies appears somewhat delayed at Stewartby, occurring some distance
389 above the base of the Grossouvrei Subzone. Scattered through the succession are relatively thin (ca.
390 1 m or less) organic-rich mudstone units identified by Duff (1975) as *Grammatodon*-rich Bituminous
391 Shale, with apparently no consistent relationship to NERC biofacies clusters, and containing
392 relatively low proportions of *Bositra* and *Meleagrinnella* and high concentrations of deposit-feeding
393 and infaunal suspension-feeding bivalves (particularly *Grammatodon*, nukulacean bivalves and the
394 gastropod *Procerithium*). Apart from these horizons, *Grammatodon* is absent from most of the
395 Peterborough Member.

396 Overall, the results suggest that there are strong site-specific factors influencing the
397 composition and successions of biofacies, with stratigraphical persistence of the distinct character of
398 sites suggesting that this pattern is not a consequence of chance variation in palaeoecological
399 conditions. Detailed results of biofacies analysis for individual boreholes are discussed below in the
400 context of environmental interpretations.

401 **4.5 Biozonal data**

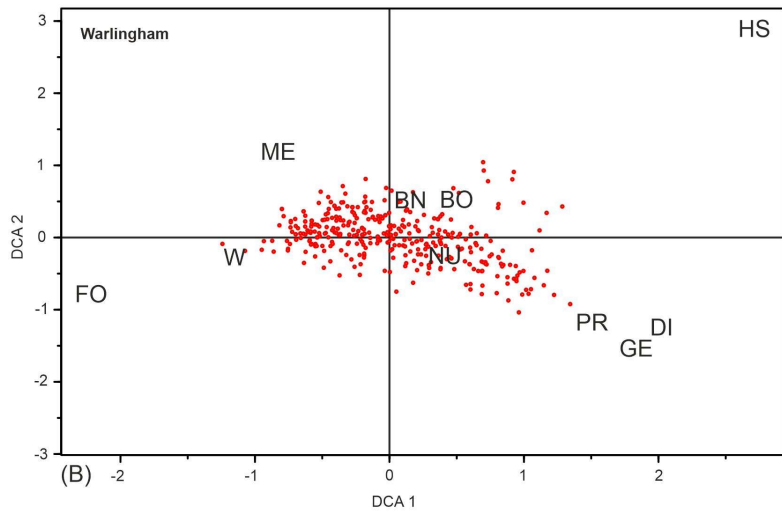
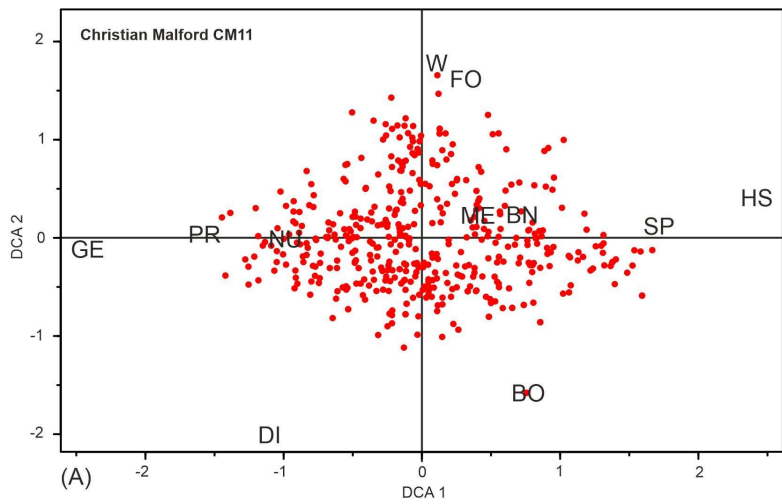
402 Compilation of biozonal data for the Peterborough Member (Fig. 10) in boreholes extending along
403 the same NE – SW alignment as our model thickness data reveals: 1) SW thickening is largely driven
404 by expansion of biozones in the lower part of the Peterborough Member; 2) the Eriswell Borehole,
405 located close to the ABM, shows maximum thinning of biozones, but expansion north-eastwards
406 away from this structural feature and towards the East Midlands Shelf and Southern North Sea is
407 muted, with the thickness of the Coronatum Zone in the Tydd St Mary and Parson Drove boreholes
408 similar to Eriswell.

409 **5 Discussion**

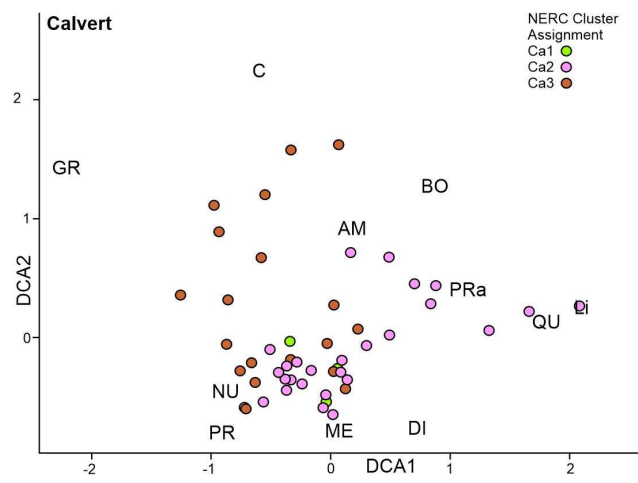
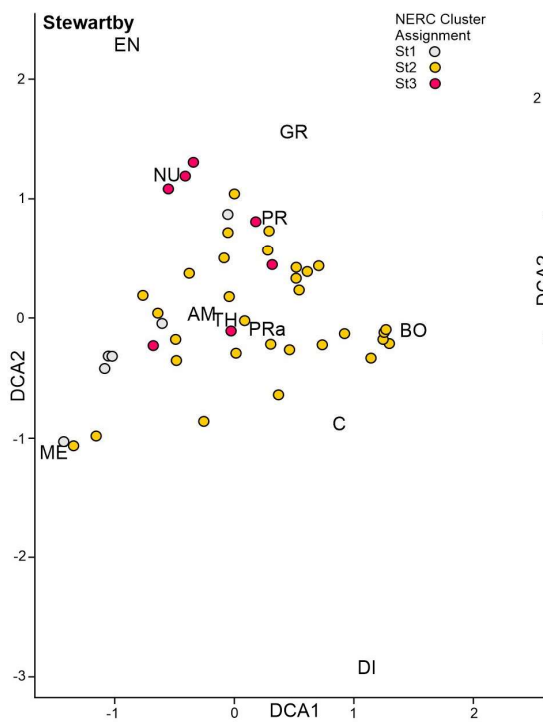
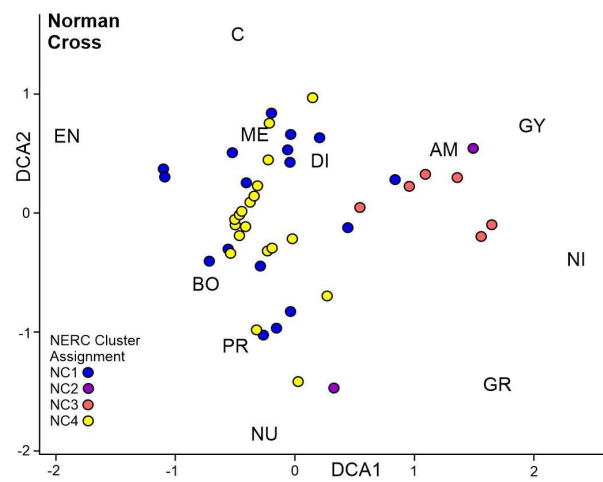
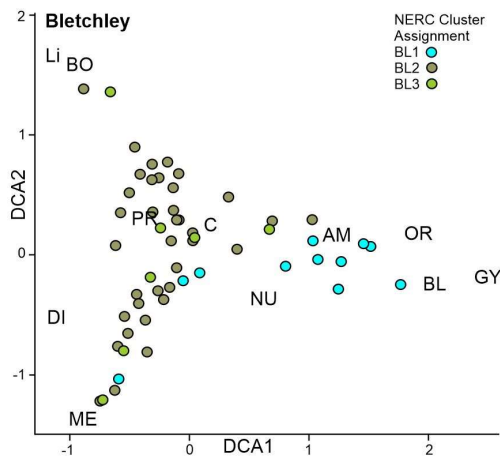
410 To understand the degree and likely causes of facies heterogeneity in the Peterborough Member
411 we: 1) use our modelled thickness data to resolve depositional geometry in the context of basin
412 structure and palaeogeography; 2) review existing sequence stratigraphy understanding for the
413 Peterborough Member in light of our new geochemical and regional biostratigraphical data to
414 establish a framework for understanding sea level variability, and 3) combine knowledge of (1) and
415 (2) to develop a conceptual basin model that explains contrasts and similarities in biofacies patterns,
416 and the extent to which they reflect basin-scale trends in mudstone variability. Finally, we make
417 comparisons with other well-known organic-rich Jurassic mudstone successions.

418 The constituent taxa of our biofacies have been the subject of previous work to understand
419 patterns of ecological change in the Peterborough Member, which are primarily controlled by
420 seabed oxygenation and/or substrate consistency (Duff 1975, Martill et al. 1994, Kenig et al. 2004).

421



422 **FIGURE 8**



424 Since our biofacies carry an ‘averaged’ environmental signal, our ecological conceptualisation of
425 them (below) is necessarily simplified, effectively dampening short-term environmental “noise”.
426 Here, we follow previous authors (Kauffman 1981, Etter 1996; Caswell et al. 2009; Danise et al.
427 2015) in regarding *Bositra* and *Meleagrinnella* as opportunist suspension feeding taxa, tolerant of low
428 oxygenation. In the context of previous work by Kenig et al. (2004) using geochemical data to
429 understand environmental signals in the biofacies of the Peterborough Member, and the
430 relationship of biofacies to Ti/K data in the CM11 succession, end-members (4.4 above) represented
431 by (1) *Bositra* -rich organic mudstone and (2) nukulacean shell beds (+/- *Procerithium*, *Genicularia*)
432 are interpreted to correspond with low oxygen (anoxic or dysoxic) and more oxygenated (oxic)
433 settings, respectively. *Meleagrinnella*-dominated successions appear to occupy a position between
434 these two end members.

435 5.1 Basin geometry and palaeogeography

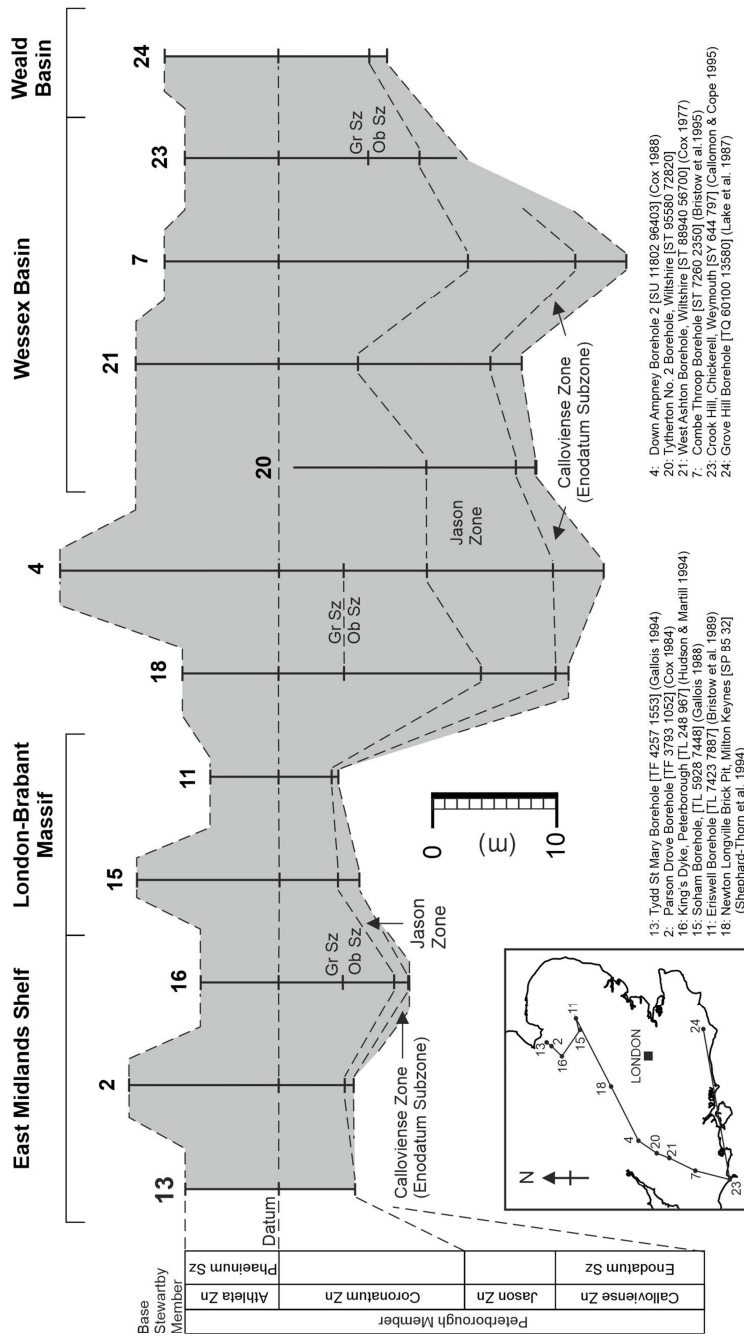
436 Modelled thicknesses reveal clear trends in the depositional pattern of the Peterborough Member,
437 with distinctly wedge-shaped regional thickness geometries characterising the unit and wider Oxford
438 Clay along the northern edge of the ABM, from the Southern North Sea into the Wessex Basin (Fig.
439 3), as well as from the eastern Weald westwards (Fig. 4). However, the palaeogeographical settings
440 of these two regions are strongly contrasting in terms of likely sediment accommodation space (Fig.
441 1), suggesting that the similar geometries are a product of different processes. Along the northern
442 margin of the ABM, north-eastward thinning closely corresponds with flanks of the Mid North Sea
443 High, and the modelled thickness variation (Fig. 3A) seems consistent with a palaeobathymetric
444 gradient from relatively shallow water conditions around this semi-emergent feature to deeper
445 water conditions in the Wessex Basin. Certainly, there is evidence in the younger Corallian Group for
446 the margins of the Mid North Sea High being associated with the development of shallow-water
447 facies (Cameron et al. 1992), and it seems probable that prior to this the broad area of crust affected
448 by North Sea doming (>1250 km diameter; Underhill and Partington 1993) extended to the East
449 Midlands Shelf during deposition of the Peterborough Member.

450 Modelled thinning of the Peterborough Member and total Oxford Clay Formation across
451 much of the Weald Basin is striking and consistent with biozonal data from cored boreholes (Fig. 10),
452 including the Grove Hill [TQ 6008 1359] and Brightling No. 1 [TQ 6725 2182] boreholes in Sussex
453 (Lake et al. 1987). This sharply contrasts with the significant thickening seen in this area during
454 deposition of the prior Inferior and Great Oolite groups and subsequent Late Jurassic succession
455 (Whittaker 1985). The conclusion from our modelling is that this area is likely to have been relatively
456 sediment starved.

457 From the thick successions of Peterborough Member in the Wessex Basin there is evidence
458 of a slight thinning trend into the Channel Basin, particularly seen in the pattern of biozonal data for
459 Dorset (Fig. 10). This may reflect greater ability of the Wessex Basin to create additional
460 accommodation space through sediment loading, with some differential compaction across fault
461 lineaments potentially suggested by thickness data in the vicinity of the Shrewton Borehole (Fig. 3C).

462 5.2 Cyclicity and Sequence Stratigraphy

463 New geochemical data for Christian Malford, and its relationship to lithological features in borehole
464 core (Fig. 5), allows interpretation of likely patterns of relative sea level change during this time.
465 Combined with our basin-wide synthesis of biostratigraphical data (Fig. 10), and previously reported
466 observations of Mid/Late Callovian successions in the wider UK region (including data for the Moray
467 Basin), we outline a sequence stratigraphy framework for the Peterborough Member that can be
468 used to understand controls on the pattern of deposition and potentially also decimetre-scale trends
469 in biofacies data. Whilst often considered as a separate depositional entity, the succession



- 13: Tydd St Mary Borehole [TF 4257, 1553] (Gallois, 1994)
- 2: Parson Drove Borehole [TF 3793, 1052] (Cox, 1984)
- 16: King's Dyke, Peterborough [TL 248, 967] (Hudson & Martill, 1994)
- 11: Kotham Borehole, [TL 2023, 7887] (Gallois, 1994)
- 14: Ewell Borehole, [TL 2023, 7887] (Gallois, 1994)
- 18: Newton Loughville Brick Pit, Milton Keynes [SP 85 32] (Shephard-Thorn et al., 1984)
- 4: Down Ampney Borehole 2 [SU 11802, 96403] (Cox, 1988)
- 20: Tytheron No. 2 Borehole, Wiltshire [ST 86940, 72820]
- 21: West Ashton Borehole, Wiltshire [ST 86940, 36700] (Cox, 1977)
- 7: Cranborne Wood Borehole [ST 7269, 54] (Cox, 1988)
- 23: Cranborne Wood Borehole [ST 7269, 54] (Cox, 1988)
- 24: Grove Hill Borehole [TQ 60100, 13590] (Lake et al., 1987)

470 FIGURE 10

471 developed on the margin of the Moray Basin (at Brora) shows noted similarity with that of eastern
472 England (Page 2002); there is broad coincidence in the stratigraphical horizon of intervals showing
473 particular sequence stratigraphical responses (e.g. progradation, maximum flooding), and
474 palaeogeographical evidence supports probable wider marine connectivity with the Oxford Clay
475 depositional system (Davies et al. 1996).

476 **5.2.1 Current knowledge framework**

477 The oldest part of the Peterborough Member, and coeval parts of the Heather and Brora
478 Argillaceous formations in the Moray Basin (Fig. 2), relate to marine flooding at the base of the
479 Enodatum Subzone and regression in the overlying Jason Zone (Davies et al. 1996, Nagy et al. 2001,
480 Hesselbo 2008). At the type Peterborough section, initial flooding and later sea level fall corresponds
481 with the 'Gryphaea and Reptile Beds', comprising a thin (1.2 m) unit of fissile pyritic mudstone rich in
482 the oyster *Gryphaea*, consistent with shallow water oxic conditions (Duff 1975, Hudson and Martill
483 1994, Kenig et al. 2004). Maximum Flooding surfaces are usually associated with thickening of the
484 associated stratigraphical intervals towards the basin margins where sediment becomes ponded on
485 newly created shelf areas (Catuneanu et al. 2011). The thin Enodatum Subzone at Peterborough
486 (compared to more basinal setting; Fig 10) suggests either a *very* proximal setting at the maximum
487 extent of flooding, and/or significant erosion associated with later sea level fall.

488 Thickening of the Jason Zone into the Wessex Basin (Fig. 10) is consistent with relative sea
489 level fall focussing sedimentation towards available accommodation space in more distal areas. In
490 this context, organic-rich facies in the higher part of the Jason Zone at Peterborough (Bed 10 of
491 Hudson and Martill 1994), sandwiched between *Gryphaea*-rich intervals, probably reflects the
492 development of anoxia in a relatively shallow water setting, possibly in response to restricted local
493 circulation (ponding, boosting organic matter preservation) associated with sea level fall. Sandstone
494 in the likely Jason Zone at Stewartby (Bedfordshire), ca. 60 km to the south-west, is interpreted to
495 reflect winnowing or bypass of fine-grained sediment in a more proximal setting (Macquaker 1994),
496 providing further evidence of limited local sediment accommodation space close to the basin margin
497 at this time.

498 Relative sea level fall is inferred to have continued into the early Coronatum Zone before
499 rising in the later part of the Zone (Hesselbo 2008). In the Moray Basin this phase is represented by a
500 wedge of coarse, glauconitic sandstone (Nagy et al. 2001), and by stacked parasequences in the
501 Peterborough succession showing a trend of increasing up-section silt content (Macquaker and
502 Howell 1999). These successions may be a response to lack of accommodation space caused by
503 relative sea level fall, and/or reflect the rapid advance of sediment into limited areas of newly
504 created accommodation space during early transgression.

505 **5.2.2 Completing the knowledge framework**

506 The remainder of the Peterborough Member reflects rising relative sea level, peaking in the lower
507 part of the Phaeinum Subzone (Hesselbo 2008) and consistent with a widespread Maximum
508 Flooding Surface recognised in the Moray Basin (Davies et al. 1996, Nagy et al. 2001). Trends in the
509 Ti/K data from the Christian Malford Borehole CM 11 are a proxy for the delivery of coarse detrital
510 components to the depositional site, and shed new light on the pattern of environmental change
511 represented by the upper part of the Peterborough Member. We regard the regular cyclical pattern
512 of Ti/K data in the Christian Malford succession (Fig. 5) as analogous to the systematic trends in the
513 silt-content used by Mcquaker (1994) and Mcquaker and Howell (1999) to understand fluctuations in
514 the length of sediment transport pathways between source and sink caused by relative sea level
515 change. Individual cycles fine-up (Type 1 cycle) or coarsen-up (Type 2 cycle) and can be grouped into
516 broader associations showing overall reductions in Ti/K or overall increases in Ti/K. These broader

517 cycle trends, and the inflection points between these trends are used to infer likely changes in
518 sediment accommodation space and to make interpretations of sequence stratigraphy.

519 The decline in the Ti/K ratio in the lowest ca. 1 m of the CM11 succession (Grossouvrei
520 Subzone; Fig. 5), terminating abruptly at a peak in the Ca/K ratio ('C' of Fig. 5) suggests that an
521 increase in accommodation space acted to reduce the flux of detrital material to this site. The
522 conspicuous ammonite/foraminifera concentration at 'C' likely represents a period of sharply
523 reduced sedimentation rate in response to sea level rise. Three cycles in the Ti/K ratio (S1 – 3, Fig. 5)
524 in the overlying ca. 1.5 m of mudstone correspond with alternating paler and darker grey mudstone
525 units, and show an overall upward increase in Ti/K. This trend through cycles S1 – 3 suggests
526 progressively enhanced delivery (progradation) of coarser-grade sediment to the depositional site
527 associated with shortening of sediment pathways. These are analogous to the parasequences
528 described in the lower part of the Peterborough succession by Macquaker and Howell (1999). The
529 largest peak (S3, Fig. 5) in Ti/K marks the beginning of a sharp upward shift to significantly lower Ti/K
530 values that persists through several metres of the overlying succession. This peak is interpreted to
531 represent a major pulse of marine transgression associated with current winnowing on newly
532 flooded areas and significant increase in available accommodation space.

533 The four closely spaced Type 1 cycles (see above) in CM11, corresponding with peaks S4 – S7
534 (Fig. 5), are interpreted to represent a series of transgressive pulses, initially marked by sediment
535 winnowing events, separated by periods with less current scour. The overall reduction in the Ti/K
536 ratio through this interval is consistent with an increase in accommodation space and lengthening of
537 sediment pathways. The major Ti/K peak (S4) associated with the lowest shell bed suggests that this
538 was a particularly strong/prolonged pulse of transgression. It coincides with a major shift in
539 biofacies, a sharp upward decline in the abundance of wood potentially reflecting increased distance
540 from shorelines, and a decline in foraminifera that is a possible response to increased current scour
541 (Fig. 5). Sharp/erosive ('X' Fig. 5) bases to the shell beds are consistent with significant current scour
542 which was probably important for oxygenation and colonisation of seabed sediment by the infaunal
543 bivalves that dominate these units. Minor Ti/K peaks (S5 – 7; Fig. 5) that cap subsequent shell beds
544 suggest a phase of enhanced off-shelf movement of mobile sediment from newly flooded areas by
545 wave scour following each transgressive pulse (including material swept across the site into more
546 distal settings). The alternation of shell-rich units and intervening mudstone is matched by a
547 pronounced oscillation in biofacies (Fig. 5). The less diverse fauna, dominated by foraminifera and
548 the bivalves *Bositra* and *Meleagrinnella*, in the dark, fissile units that cap the cycles, suggests quieter
549 depositional conditions with less consistent sea bed oxygenation. The Comptoni Bed (peak S8),
550 widely associated with a rolled and winnowed fauna (Hudson and Martill 1994), is inferred to mark
551 the maximum extent of transgression, and therefore the Maximum Flooding Surface.

552 Above the Acutistriatum Band in CM11, the progressive cyclical build-up in Ti/K (Fig. 5, S9 –
553 S14), indicates a major shift in basin evolution. Biofacies at and just above the Acutistriatum Band
554 (and particularly between peaks S9 & S10) are indicative of dysoxic conditions (enrichment in
555 *Bositra*, coprolite) and are consistent with low sedimentation rates (enrichment in bone), and the
556 Acutistriatum Band is interpreted as a Condensed Section at the base of a Highstand Systems Tract
557 (cf. Catuneanu et al. 2009). The stacked succession of Type 2 cycles (see above) with progressively
558 increasing detrital content that form the remainder of the succession in CM11 and overlapping parts
559 of CM9 are interpreted to form part of a 'normal regression' (Catuneanu et al. 2011) during sea level
560 Highstand. Peaks S11 – 15 (Fig. 5), and likely represent the winnowed tops of prograding
561 parasequences, represented by paler and generally more shell-rich mudstone units in borehole core.
562 Reducing amplitude of Ca/K peaks upwards through the interval is probably a response to increasing
563 dilution of shell by sediment influx, whilst the gradational bases of shell beds ('Y' Fig. 5) might reflect
564 the ability of infauna colonising parasequences to progressively improve the habitability of deeper

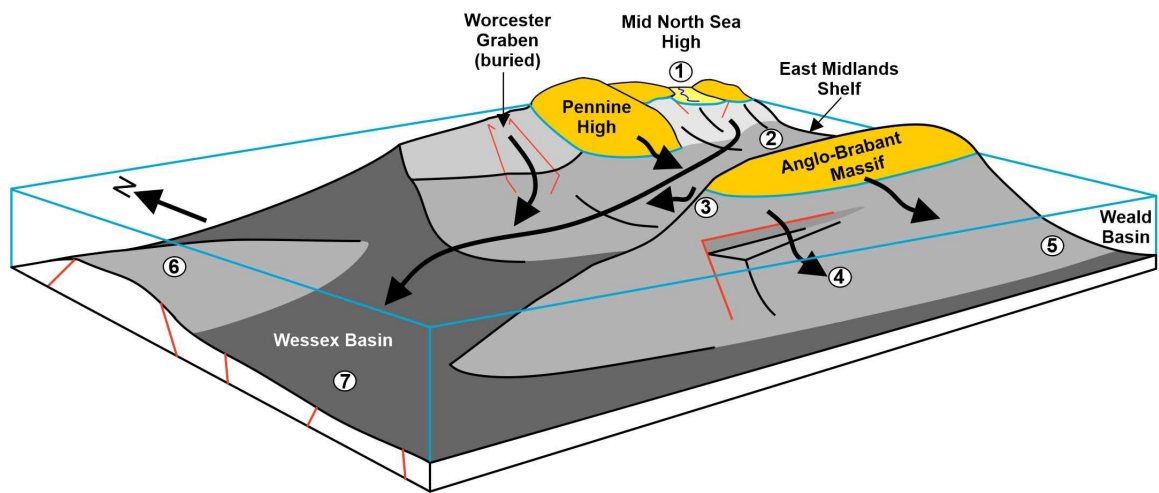
565 sediment layers by improving oxic water circulation. Decimetre-thick intervals of dark, organic-rich,
566 fissile mudstones, that are either sparsely shelly or dominated by *Bositra* and ammonites, represent
567 periods of deposition when creation of new accommodation space (e.g. from minor sea level
568 fluctuation or basin subsidence) outstripped sediment flux, and current circulation was less effective
569 at maintaining seabed oxygenation. Initially, the Type 2 cycles are poorly defined by biofacies data,
570 but around the 'Squid Bed' (Fig. 5) and coincident with the horizon of the Christian Malford
571 *Lagerstätte* (Wilby et al. 2008), the distinction of *Bositra*-rich intervals suggests an increasing trend
572 towards anoxia/dysoxia. Plateauing of Ti/K values above S14 potentially reflects over-extension of
573 sediment pathways, and diversion of material to adjacent regions with steeper shelf to basin
574 gradients.

575 **5.3 Conceptual basin model and mudstone heterogeneity**

576 Modelled thickness data for the Peterborough Member, combined with knowledge of the
577 palaeogeographical framework for the Mid Callovian (Figs. 1, 3), suggest that a depth gradient from
578 the Mid North Sea High, and laterally contiguous areas, was likely significant in focusing sediment
579 south-westwards towards the Wessex Basin, potentially augmented by sediment flows via the
580 Worcester Graben. Palaeocurrent data for the Oxford Clay are sparse, but Hudson and Martill (1991)
581 speculated that a large assemblage of belemnites seen at Peterborough (>300 specimens; Martill,
582 1985) with a N – S alignment might reflect the action of currents responsible for removing sediment
583 from the East Midlands Shelf succession and depositing it in deeper parts of the basin. In the Mid
584 Callovian, the Mid North Sea High formed an extensive semi-emergent area arcing around the
585 southern North Sea Basin, with a coal-forming deltaic system in the Central North Sea (Møller and
586 Rasmussen 2003), both providing significant potential for delivery of fine-grained sediment to
587 offshore regions (Fig. 11). Thin and significantly condensed sedimentation on the flanks of the ABM
588 (Figs. 3, 10) suggests that even if not fully emergent, it likely formed a significant structural feature.
589 However, similarly thin Peterborough Member successions in the Weald Basin, where sediment
590 accommodation space is unlikely to have been limited, suggest sediment starvation, with limited
591 supply of sediment from the ABM itself and likely shielding by the ABM from sediment sources
592 further north.

593 In the Wessex Basin, the thick Peterborough Member potentially includes material fed via
594 the Worcester Graben (Fig. 11), which structural and regional gravity data (Chadwick and Evans,
595 2005; Fig. 12) suggest was a long-lived conduit for Mesozoic sediments. Published data for the
596 source of Oxford Clay sediments are lacking, but it is noticeable that thickening of the Peterborough
597 Member occurs in geophysical log transects across the buried mouth of this structure, located north
598 of the current outcrop margin (Fig. 12). Maintenance of accommodation space in the Wessex Basin
599 was probably a response of the highly fractured basement to the extensional stresses responsible for
600 North Sea rifting, coupled with greater potential for compactional subsidence of the thick underlying
601 Triassic and Early Jurassic succession, in contrast to the shallow-buried Variscan basement on the
602 East Midlands Shelf (Whittaker 1985, Map 3).

603 The inferred patterns of sea level change are reflected by variable litho- and bio-facies
604 across the basin, that appears largely a response to local basin setting. Thus, sea level fall in the
605 Jason Zone is associated with the development of organic-rich mudstone in probable shallow water
606 settings on the East Midlands Shelf, whereas coeval strata at Combe Throop and Kimmeridge 2, in
607 the Wessex Basin, contain relatively low proportions of *Bositra*, and high proportions of oysters,
608 nuculacean bivalves and the deep burrowing bivalve *Thracia* (Fig. 6), indicative of broadly oxic
609 conditions. Higher in the succession, sea level rise across the Coronatum/Athleta Zone boundary is
610 reflected by a shift to more organic-rich facies at Christian Malford. Further south-west in the
611 Wessex Basin, correlative strata at Combe Throop comprise silty laminated sediments characterised



612 **FIGURE 11**

613 by high proportions of both *Bositra* and nuculacean bivalves (Fig. 6), suggesting more rapidly
614 fluctuating oxic/suboxic/anoxic environments. This plausibly reflects the position of the borehole on
615 the Hampshire – Dieppe High, and perhaps also contrasting conditions affecting the fault-bounded
616 Mere Basin opening immediately to the north (Chadwick and Evans 2005, fig. 85).

617 In the Down Ampney 2 Borehole, 30 km NE of CM11, laminated mudstone facies in the
618 lower part of the Phaeinum Subzone (Fig. 6) contains common wood, bone and foraminifera, but
619 few other fossil remains. The abundance of wood and bone in laminated mudstone facies suggests
620 low rates of sedimentation in a low energy, near-shore setting. The general absence of biota might
621 indicate significant localised freshwater run-off affecting both salinity and potentially also
622 oxygenation. This unusual and unique unit suggests significant influence of local
623 basin/environmental factors. It occurs between two contrasting successions: dark grey laminated
624 bioclastic mudstone in the early Phaeinum Subzone (with biofacies dominated by *Bositra*,
625 *Meleagrinnella* & nuculacean bivalves) suggesting an intermittently dysoxic marine setting, and pale
626 grey, poorly laminated and conspicuously bioturbated silty and shelly mudstone above (with
627 biofacies dominated by nuculaceans, *Procerithium*, foraminifera and subsidiary *Bositra*), suggesting
628 more, oxic, open marine circulation.

629 In the Parson Drove Borehole on the East Midlands Shelf, biofacies clusters with high
630 proportions of *Bositra* dominate much of the succession, suggesting a persistent pattern of low
631 oxygenation (Fig. 6). Pale grey, silty mudstone facies that dominate most of the Phaeinum Subzone
632 in the Down Ampney succession, only occur near the top of the Phaeinum Subzone in the Parson
633 Drove succession. This interpretation is supported by the sparse record of *Genicularia* in much of the
634 Parson Drove succession, seen also in the voluminous quantitative data of Duff (1974, 1975) collected
635 from the East Midlands Shelf. *Genicularia* is an epifaunal suspension feeding serpulid (Duff, 1975)
636 that our biofacies data show is predominantly associated with strongly developed nuculacean shell
637 beds. On DCA data plots (Fig. 8) *Genicularia* is consistently distant from poles defined by fauna linked
638 to dysoxic environments (e.g. *Bositra*, *Meleagrinnella*), and Duff (1975) recorded it as a dominant
639 component in his calcareous clay facies, characterised by a diverse fauna including nuculaceans and
640 oysters and low Total Organic Carbon (TOC). With these characteristics, we regard *Genicularia* in our
641 biofacies data as an indicator of some of the least dysoxic conditions in the Peterborough Member.
642 In the Parson Drove Borehole, *Genicularia* is present towards the top of the succession, coincident
643 with a shift to much paler grey, silty mudstone (Fig. 6), potentially presaging wider regional
644 environmental change in the later part of the Athleta Zone.

645 The sporadic distribution of the *Grammatodon*-rich Bituminous Facies of Duff (1975), and its
646 unusual fauna dominated by elements more typical of oxic conditions is enigmatic. Duff (1974)
647 suggested that this facies was likely associated with a slight increase in current activity, and many
648 modern arcid bivalves (like *Grammatodon*) are adapted to life in unstable environments from which
649 they might be dislodged by currents (Thomas 1978). Such an environment seems unfavourable for
650 the build-up of significant organic enrichment (up to 6.1% TOC; Duff, 1974), unless this was prolific
651 and occurred in periods of relatively short duration (e.g. linked to disturbance of redox boundaries
652 across the East Midlands Shelf by enhanced storm activity).

653 Significant contrasts with the East Midlands Shelf and Wessex Basin occur in the facies at the
654 margin of the ABM at Eriswell, and at Warlingham on the edge of the Weald Basin. At Eriswell,
655 biofacies are consistently rich in broken-up shell material and generally poor in ammonites, where
656 current winnowing in a relatively shallow water setting likely shaped deposition of the thin and
657 condensed succession. The large number of faunal clusters might reflect the development of cryptic
658 omission surfaces separating units with subtly varying faunal composition. Here, the relative rarity of
659 *Genicularia* is unexpected in a setting that evidence suggests was likely well oxygenated, and may be
660 a response to the high energy marine setting. The main facies response to rising sea level at the base

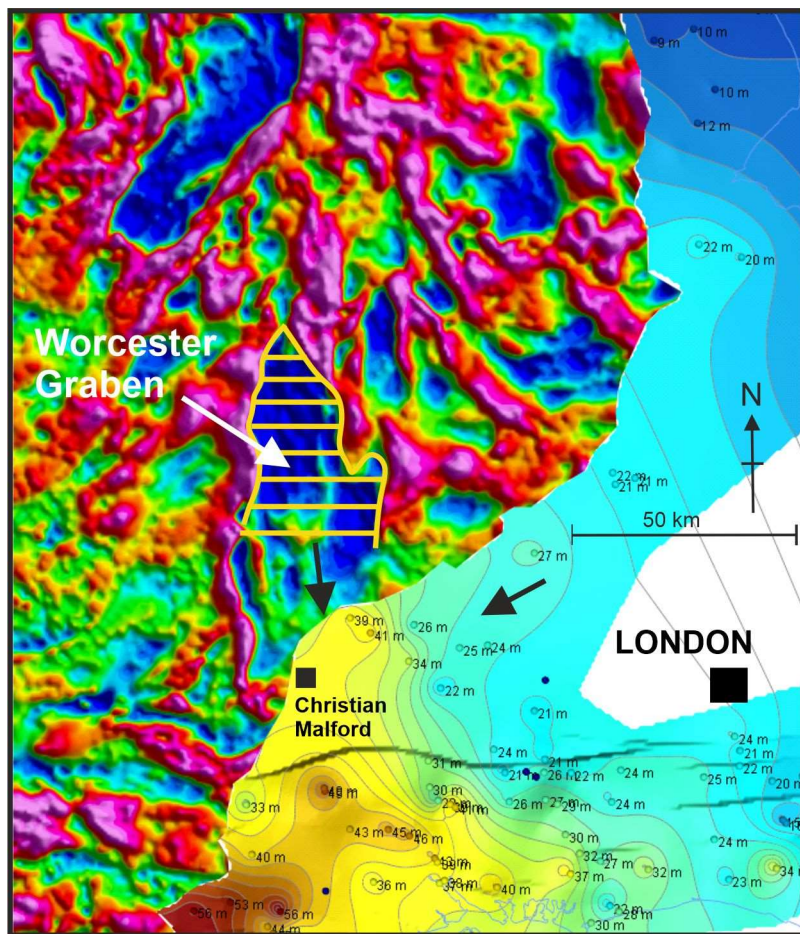
661 of the Athleta Zone in the Eriswell succession is a slight increase in the frequency of ammonites as
662 marine deepening likely strengthened connectivity with open marine settings. In contrast,
663 *Genicularia* is unusually abundant in the Athleta Zone in the Warlingham succession (CL3, Fig. 6),
664 where the DCA plot and the composition of biofacies clusters (Fig. 6, 9B) show that *Bositra* and
665 nuculacean bivalves are closely associated and present in high proportions throughout the
666 succession. Here, inferred sea level rise across the Coronatum/Athleta Zone boundary is marked by a
667 subtle change in biofacies composition, largely related to the disappearance of the bivalve
668 *Meleagrinnella* in the lower part of the *Athleta* Zone. A similar gap in the record of this bivalve is
669 noticeable at other sites (e.g. Eriswell, CM11, Combe Throop), and is likely driven by factors that are
670 not site specific. Thus, at Warlingham, the significance of this bivalve for defining a change in
671 biofacies at the Coronatum/Athleta Zone boundary is largely an indication of the unusual
672 compositional stability of other biofacies components through much of the succession. High
673 concentrations of bone suggest low sedimentation rates and/or in situ sediment winnowing
674 (Boessenecker et al. 2014) causing mixing of faunal components. This process may have been helped
675 by export of winnowed sediment from the adjacent ABM, potentially aided by Callovian syn-
676 depositional normal faulting at the margin of the Weald Basin (Holloway 1985), creating a steep
677 sediment pathway. Further out into the Weald Basin the conditions influencing deposition are
678 unclear. The thin succession and evidence of pyritic and organic-rich lithologies rich in *Bositra* and
679 bone seen in Ashdown 2 Borehole, suggest a poorly oxygenated, sediment starved setting.

680 **6. The Peterborough Member in context**

681 Facies patterns in the Peterborough Member appear more laterally variable than other organic-rich
682 Jurassic mudstone units in SE Britain, like the underlying Lias Group and overlying Kimmeridge Clay
683 Formation (Wignall 1991, Taylor et al. 2001), in which depositional patterns are predominantly
684 modulated by Milankovitch climate cycles (Weedon et al., 2004, Pearce et al. 2010, Xu et al. 2017) or
685 major oceanographic change (Toarcian Oceanic Anoxic Event (OAE); McArthur et al. 2008). The
686 evidence from this work is that basin palaeogeography produced a more laterally variable response
687 of facies in relation to relative sea level change in the Peterborough Member. This facies variability
688 may, at least in part, reflect the timing of deposition of the Peterborough Member, which occurred
689 at a relatively early stage in a cycle of broader sea level rise following rifting, potentially providing a
690 more dynamic and accentuated basin environment for its deposition compared to other Jurassic
691 mudstones. The contrasting development of organic-rich mudstones in the lower Phaeinum
692 Subzone at Christian Malford, compared to some more distal parts of the Wessex Basin, might not
693 only reflect the influence of complex structure transecting the basin; it might also indicate that
694 shallower regions of the basin margin more easily became thermally stratified and anoxic. This is
695 somewhat analogous to transgressive nearshore black shales described by Wignall and Newton
696 (2001) in the Kimmeridgian, and by Leonowicz (2016) in the Middle Jurassic of Poland, although the
697 Christian Malford organic mudstone succession appears to represent deposition during early
698 Highstand and also in a more distal, though not basinal, setting.

699 Although some previous workers have characterised the Callovian as an OAE (Hautevelle et
700 al. 2006, Souza 2014), widespread deposition of organic-rich facies (Dromart et al. 2003, Martinez
701 and Dera 2015) appears more strongly related to continental rifting (Robertson and Ogg 1986) and
702 the creation of intra-shelf basins (Carrigan et al. 1995). These widely distributed but more localised
703 tectonic settings, coupled with marine transgression and a nutrient supply fed by humid climate
704 weathering, seem likely to have been controlling influences in both organic matter accumulation in
705 the Callovian, and the demise of contemporary shallow-water carbonate platforms (Hautevelle et al.
706 2006, Andrieu et al. 2016).

707



708 **FIGURE 12**

709

710 Termination of Callovian organic matter sequestration that defines the Peterborough
 711 Member coincides with evidence of southward migration of polar and sub-polar waters across the
 712 Eur-Russian area and a major shift in the Late Jurassic climate system (Dromart et al. 2003, Dera et
 713 al. 2015). This may have been a consequence of carbon-burial and CO₂ draw-down (Dromart et al.
 714 2003), or potentially in response to the impact of rifting on patterns of marine circulation.

715 **7. Conclusions**

716 Deposition of the Peterborough Member was likely strongly influenced by highly variable basin
 717 architecture, with a depositional gradient from the Mid North Sea High channelling sediment
 718 towards the Wessex Basin, and the Anglo-Brabant Massif acting to shield the Weald Basin from this
 719 sediment source. Deposition on the flanks of the ABM is thin and condensed, and limited in the
 720 Weald Basin, suggesting sediment starvation, despite the likely presence of significant sediment
 721 accommodation space.

722 The facies at given points in the basin reflect the impact of local basin architecture and its
 723 interplay with variable sea level. Spatial contrasts in facies across the basin provide evidence of
 724 environmental gradients that can be used to inform how these facies are likely to be distributed and
 725 transition across the basin. For example, organic-rich mudstones on the East Midlands Shelf in the
 726 Jason Zone, coincident with low relative sea level, correspond with biofacies in the Wessex Basin

727 indicative of relatively greater oxygenation, with significant silt content, and containing limited
728 lithological evidence for poor circulation. The facies response of the Peterborough Member to
729 relative sea level rise at the base of the Athleta Zone is markedly variable. At the edge of the Wessex
730 Basin there is a sharp transition into organic-rich mudstone with a sparse fauna of infaunal bivalves;
731 further into the Wessex Basin the signal is much less stark, with no sustained facies shift, but instead
732 evidence of rapid oscillation between more and less oxic facies; and at the margin of the Weald
733 Basin the event occurs within a shell-rich interval, with components indicative of a range of
734 environments, that may reflect the impact of steep (?fault-controlled) depositional gradients.

735 Compared to other organic-rich mudstones, like the Kimmeridge Clay Formation, the
736 Peterborough Member seems to be a product of a much more heterogeneous depositional
737 environment. This may reflect deposition at an early stage in the cycle of regional sea level rise
738 combined with the continued impact of earlier regional uplift, both potentially acting to restrict
739 accommodation space (Macquaker, 1994) and accentuate the impact of basin irregularity on facies
740 patterns. Given the broad and varied character of the successions investigated for this work, the
741 location of the stratotype Peterborough Member appears unrepresentative of conditions across the
742 wider depositional basin. It cautions against developing basin-scale models from a few well exposed
743 and heavily researched outcrop successions, and emphasises the value of multidisciplinary studies
744 for revealing the underlying depositional controls that shape the geometry and complexity of
745 mudstone heterogeneity.

746 **Acknowledgements:** We thank J D Hudson (University of Leicester), M J Norry (formerly University
747 of Leicester) and S G Molyneux (BGS) for useful discussion and comment, and K N Page (University of
748 Exeter) and M J Barron (formerly BGS) for providing advice on stratigraphy and correlation. We
749 particularly acknowledge the contribution of our former colleague B M Cox for the wealth of data on
750 the fauna and stratigraphy of the Oxford Clay published in BGS Technical Reports. We also
751 acknowledge the United Kingdom Oil and Gas Authority (<https://www.ogauthority.co.uk/>) for
752 allowing use of borehole geophysical log data. This paper is published with the permission of the
753 Executive Director, British Geological Survey, UKRI.

754

755

756 **References**

- 757 Andrieu, S., Brigaud, B., Barbarand, J., Lasseur, E., & Saucède, T. (2016). Disentangling the control of
758 tectonics, eustasy, trophic conditions and climate on shallow-marine carbonate production during
759 the Aalenian – Oxfordian interval: From the western France platform to the western Tethyan
760 domain. *Sedimentary Geology*, *345*, 54 – 84.
761
- 762 Birgenheier, L. P., Horton, B., McCauley, A. D., Johnson, C. L., & Kennedy, A. (2017). A depositional
763 model for offshore deposits of the lower Blue Gate Member, Mancos Shale, Uinta Basin, Utah, USA.
764 *Sedimentology*, *64*, 1402 – 1438.
765
- 766 Boessenecker, R. W., Perry, F., & Schmitt, J. G. (2014). Comparative Taphonomy, Taphofacies, and
767 Bonebeds of the Mio-Pliocene Purisima Formation, Central California: Strong Physical Control on
768 Marine Vertebrate Preservation in Shallow Marine Settings. *PLOS ONE*
769 <https://doi.org/10.1371/journal.pone.0091419>.
770
- 771 Bradshaw, M. J., Cope, J. C. W., Cripps, D. W., Donovan, D. T., Howarth, M. K., Rawson, P. F., West, I.
772 M., & Wimbledon, W. A. (1992). Jurassic. In Cope, J. C. W., Ingham, J. K. & Rawson, P. F. (Eds.), *Atlas*
773 *of Palaeogeography and Lithofacies, Geological Society Memoir*, *13*, 107 – 129.
774
- 775 Bristow, C. R., Barton, C. M., Freshney, E. C., Wood, C. J., Evans, D. J., Cox, B. M., Ivimey-Cook, H. C.,
776 & Taylor, R. T. (1995). Geology of the country around Shaftesbury. *Memoir of the British Geological*
777 *Survey, 1:50 000 geological sheet 313* (England & Wales).
778
- 779 Bristow, C. R., Cox, B. M., Ivimey-Cook, H. C., & Morter, A. A. (1989). The stratigraphy of the Eriswell
780 Borehole, Suffolk. *British Geological Survey Research Report, SH/89/2*.
781
- 782 Buckley, D. K., Cripps, A. C., Barron, A. J. M., & Evans, A. D. (1991). Geophysical logging of several
783 boreholes in Marston Vale, Bedfordshire. *British Geological Survey Technical Report, WN/91/23*.
784
- 785 Butler, D. (2010). France digs deep for nuclear waste. *Nature*, *466*, 804 – 805.
786
- 787 Callomon, J. H. (1968). The Kellaways Beds and the Oxford Clay. In Sylvester-Bradley, P. C., & Ford T.
788 D. (Eds.), *The Geology of the East Midlands* (pp. 264 – 290). Leicester: University Press.
789
- 790 Callomon, J. H., & Cope, J. C. W. (1995). The Jurassic Geology of Dorset. In Taylor, P. D. (Ed.), *Field*
791 *Geology of the British Jurassic* (pp. 51 – 103). London: The Geological Society.
792
- 793 Callomon, J. H., & Cope, J. C. W. (1971). II. – The stratigraphy and ammonite succession of the Oxford
794 and Kimmeridge Clays in the Warlingham Borehole. *Bulletin of the Geological Survey of Great Britain*,
795 *36*, 147 – 168.
796
- 797 Carrigan, W. J., Cole, C. A., Colling, E. I., & Jones, P. J. (1995). Geochemistry of the Upper Jurassic
798 Tuwaiq Mountain and Hanifa Formation Petroleum Source Rocks of Eastern Saudi Arabia. In Katz, B.
799 J. (Ed.), *Petroleum Source Rocks* (pp. 67 – 87). Berlin, Heidelberg: Springer.
800

801 Caswell, B. A., Coe, A. L., & Cohen, A. S. (2009). New range data for marine invertebrate species
802 across the early Toarcian (Early Jurassic) mass extinction. *Journal of the Geological Society, London,*
803 *166*, 859 – 872.

804

805 Catuneanu, O., Galloway, W. E., Kendall, C. G. St. C., Miall, A. D., Posamentier, H. W., Strasser, A., &
806 Tucker, M. E. (2011). Sequence Stratigraphy: Methodology and Nomenclature. *Newsletters on*
807 *Stratigraphy*, *44*, 173 – 245.

808

809 Catuneanu, C., Abreu, V., Bhattacharya, J. P., Blum, M. D., Dalrymple, R. W., Eriksson, P. G., Fielding,
810 C. R., Fischer, W. L., Galloway, W. E., Gibling, M. R., Giles, K. A., Holbrook, J. M., Jordan, R., Kendall, C.
811 G. St. C., Macurda, B., Martinsen, O. J., Miall, A. D., Neal, J. E., Nummedal, D., Pomar, L.,
812 Posamentier, H. W., Pratt, B. R., Sarg, J. F., Shanley, K. W., Steel, R. J., Strasser, A., Tucker, M. E., &
813 Winker, C. (2009). Towards the standardization of sequence stratigraphy. *Earth Science Reviews*, *92*,
814 1 – 33.

815

816 Chadwick, R. A., & Evans, D. J. (2005). *A seismic atlas of Southern Britain*. Keyword: The British
817 Geological Survey.

818

819 Charrad, M., Ghazzali, N., Boiteau, V., & Niknafs, A. (2014). NbClust: An R Package for Determining
820 the Relevant Number of Clusters in a Data Set. *Journal of Statistical Software*, *61(6)*, 1 – 36.

821

822 Cope, J. C. W. (2006). 14 Jurassic: the returning seas. In Brenchley, P. J., & Rawson, P. F. (Eds.), *The*
823 *Geology of England and Wales* (pp. 325 – 363). London: The Geological Society.

824

825 Cox, B. M. (1991). Combe Throop Borehole, Combe Throop, Somerset, Oxford Clay. *British Geological*
826 *Survey Technical Report, WH/91/310R*.

827

828 Cox, B. M. (1990). A review of Jurassic Chronostratigraphy and age indicators for the UK. In
829 Hardman, R. F. P. & Brooks, J. (eds), *Tectonic Events Responsible for Britain's Oil and Gas*
830 *Reserves, Geological Society Special Publication*, *55*, 169-190

831

832 Cox, B. M. (1988). Fluid Processes Research Group: Down Ampney Fault Study. Stratigraphic
833 classification of boreholes. *British Geological Survey Technical Report, WH/88/182R*.

834

835 Cox, B. M. (1984). Parson Drove (West's Bridge Borehole), Cambs. *British Geological Survey Technical*
836 *Report, PDL/84/70*.

837

838 Cox, B. M. (1977). Ashton 1 Borehole. *British Geological Survey Technical Report, PD/77/22*.

839

840 Cox, B. M., Hudson, J. D., & Martill, D. M. (1992). Lithostratigraphic nomenclature of the Oxford Clay
841 (Jurassic). *Proceedings of the Geologists' Association*, *103*, 343 – 345.

842

843 Danise, S., Twitchett, R. J., & Little, C. T. S. (2015). Environmental controls on Jurassic marine
844 ecosystems during global warming. *Geology*, *43*, 263 – 266.

845

846 Davies, R. J., Stephen, K. J., & Underhill, J. R. (1996). A re-evaluation of Middle and Upper Jurassic
847 stratigraphy and the flooding history of the Moray Firth Rift System, North Sea. In Hurst, A. (Ed.),

848 Geology of the Humber Group: Central Graben and Moray Firth, UKCS. *Geological Society Special*
849 *Publication*, 114, 81 – 108.

850

851 Delay, J., Rebours, H., Vinsot, A., & Pierre, R. (2007). Scientific investigation in deep wells for nuclear
852 waste disposal studies at the Meuse/Haute Marne underground research laboratory, northeastern
853 France. *Physics and Chemistry of the Earth*, 32, 42 – 57.

854

855 Dera, G., Prunier, J., Smith, P. L., Haggart, J. W., Popov, E., Guzhov, A., Rogov, M., Delsate, D., Thies,
856 D., Cuny, G., Pucéat, E., Charbonnier, G., & Bayon, G. (2015). Nd isotope constraints on ocean
857 circulation, paleoclimate, and continental drainage during Jurassic breakup of Pangea. *Gondwana*
858 *Research*, 27, 1599 – 1615.

859

860 Dromart, G., Garcia, J.-P., Picard, S., Atrops, F., Lécuyer, C., & Sheppard, S. M. F. (2003). Ice age at the
861 Middle – Late Jurassic transition? *Earth and Planetary Science Letters*, 213, 205 – 220.

862

863 Duff, K. L. (1975). Palaeoecology of a bituminous shale – the Lower Oxford Clay of central England.
864 *Palaeontology*, 18, 443 – 482.

865

866 Duff, K. L. (1974). *Studies of the Palaeontology of the Lower Oxford Clay of Southern England*. PhD
867 Thesis, University of Leicester.

868

869 Etter, W. (1996). Pseudoplanktonic and benthic invertebrates in the Middle Jurassic Oplalinum Clay,
870 northern Switzerland. *Palaeogeography, Palaeoclimatology, Palaeoecology*, 129, 325 – 341.

871

872 Gallois, R. W. (1994). Geology of the country around King's Lynn and The Wash. *Memoir of the*
873 *British Geological Survey*, 1:50 000 Sheet 145 and part of Sheet 129 (England & Wales).

874

875 Gallois, R. W. (1988). Geology of the country around Ely. *Memoir of the British Geological Survey*,
876 1:50 000 Sheet 173 (England & Wales).

877

878 Gallois, R. W. (1979). Geological investigations for The Wash Water Storage Scheme. *Report of the*
879 *Institute of Geological Sciences*, 78/19.

880

881 Gallois, R. W., & Worssam, B. C. (1983). Stratigraphy of the Harwell Boreholes. *Institute of Geological*
882 *Sciences, Technical Report FLPU 83-14*.

883

884 Goslee, S. C., & Urban, D. L. (2007). The ecodist package for dissimilarity-based analysis of ecological
885 data. *Journal of Statistical Software* 22(7), 1 – 19.

886

887 Hart, M. B., Page, K. N., Price, G. D., & Smart, C. W. (2019). Reconstructing the Christian Malford
888 ecosystem in the Oxford Clay Formation (Callovian, Jurassic) of Wiltshire: exceptional preservation,
889 taphonomy, burial and compaction. *Journal of Micropalaeontology*, 38, 133 – 142.

890

891 Hart, M. B., De Jonghe, A., Page, K. N., Price, G. D., & Smart, C. W. (2016). Exceptional accumulations
892 of statoliths in association with the Christian Malford Lagerstätte (Callovian, Jurassic) in Wiltshire,
893 United Kingdom. *Palaaios*, 31, 203 – 220.

894 Hautevelle, Y., Michels, R., Malartre, F., & Trouiller, A. (2006). The initiation and end of a Mesozoic
895 crisis of carbonate productivity as recorded by organic geochemical proxies. Relations with oceanic
896 anoxic events and paleoclimate changes. *Geophysical Research Abstracts*, 8, 08639.

897

898 Hesselbo, S. P. (2008). Sequence stratigraphy and inferred relative sea-level change from the
899 onshore British Jurassic. *Proceedings of the Geologists' Association*, 119, 19 – 34.

900

901 Holloway, S. (1985). Upper Jurassic: early Callovian to Middle Oxfordian. In Whittaker, A. (Ed.), *Atlas*
902 *of Onshore Sedimentary Basins in England and Wales: Post-Carboniferous Tectonics and*
903 *Stratigraphy*. Glasgow: Blackie, 47 – 48.

904

905 Hudson, J. D., & Martill, D. M. (1994). The Peterborough Member (Callovian, Middle Jurassic) of the
906 Oxford Clay Formation at Peterborough, UK. *Journal of the Geological Society, London*, 151, 113 –
907 124.

908

909 Hudson, J. D., & Martill, D. M. (1991). The Lower Oxford Clay: production and preservation of organic
910 matter in the Callovian (Jurassic) of central England. In Tyson, R. V. & Pearson, T. H. (Eds.), *Modern*
911 *and Ancient Continental Shelf Anoxia. Special Publication of the Geological Society, London*, 58, 363 –
912 379.

913

914 Juggins, S. (2017). *rioja: Analysis of Quaternary Science Data, R package version (0.9-15.1)*.
915 <http://cran.r-project.org/package=rioja>.

916

917 Kauffman, E. G. (1981). Ecological reappraisal of the German Posidonienschiefer (Toarcian) and the
918 stagnant basin model. In Gray, J., Boucot, A. J. & Berry, W. B. N. (Eds) *Communities of the Past*.
919 Stroudsburg, Pennsylvania: Hutchinson Ross, 311 – 381.

920

921 Kenig, F., Hudson, J. D., Damsté, J. S. S., Popp, B. N. (2004). Intermittent euxinia: Reconciliation of a
922 Jurassic black shale with its biofacies. *Geology*, 32, 421 – 424.

923

924 Kenig, F., Hayes, J. M., Popp, B. N., & Summons, R. E. (1994). Isotopic biogeochemistry of the Oxford
925 Clay Formation (Jurassic), UK. *Journal of the Geological Society, London*, 151, 139 – 152.

926

927 Lake, R. D., Young, B., Wood, C. J., & Mortimore, R. N. (1987). Geology of the country around Lewes.
928 *Memoir of the British Geological Survey*, 1:50 000 Sheet 319 (England & Wales).

929

930 Leonowicz, P. (2016). Nearshore transgressive black shale from the Middle Jurassic shallow-marine
931 succession from southern Poland. *Facies*, 62, 16.

932

933 Lott, G. K., & Knox, R. W. O'B. (1994). 7. Post-Triassic of the Southern North Sea. In Knox, R. W. O'B.,
934 Cordey, W. G. (Eds.), *Lithostratigraphic nomenclature of the UK North Sea*. Keyworth, Nottingham,
935 UK: British Geological Survey on behalf of the UK Offshore Operators Association.

936

937 Macquaker, J. H. S. (1994). A lithofacies study of the Peterborough Member, Oxford Clay Formation
938 (Jurassic), UK: an example of sediment bypass in a mudstone succession. *Journal of the Geological*
939 *Society, London*, 151, 161 – 172.

940

941 Macquaker, J. H. S., & Bohacs, K. M. (2007). On the accumulation of mud. *Science*, 318, 1734 – 1735.

942
943 Macquaker, J. H. S., & Howell, J. K. (1999). Small-scale (<5.0 m) vertical heterogeneity in mudstones:
944 implications for high-resolution stratigraphy in siliciclastic mudstone successions. *Journal of the*
945 *Geological Society, London, 156*, 105 – 112.

946
947 Magurran, A. E. (2004). *Measuring Biological Diversity*. Oxford, UK: Blackwell Publishing.

948
949 Mallet, J. L., (1989). Discrete Smooth Interpolation. *ACM Transactions on Graphics, 8*, 121 – 144.
950 <http://dx.doi.org/10.1145/62054.62057>

951 Martill, D. M. (1985). Studies of the vertebrate palaeontology of the Oxford Clay (Jurassic) of
952 England. Unpublished PhD thesis, University of Leicester.

953
954 Martill, D. M., Taylor, M. A., Duff, K. L., Riding, J. B., & Bown, P. R. (1994). The trophic structure of the
955 biota of the Peterborough Member, Oxford Clay Formation (Jurassic), UK. *Journal of the Geological*
956 *Society, London, 151*, 173 – 194.

957
958 Martinez, M., & Dera, G. (2015). Orbital pacing of carbon fluxes by a ~9-My eccentricity cycle during
959 the Mesozoic. *PNAS, 112*, 12604 – 12609.

960
961 McArthur, J. M., Alegro, T. J., Schootbrugge, B. van de, Li, Q., & Howarth, R. J., (2008). Basinal
962 restriction, black shales, Re-Os dating, and the Early Toarcian (Jurassic) oceanic anoxic event.
963 *Paleoceanography, 23*, PA4217.

964
965 Møller, J. J., & Rasmussen, E. S. (2003). Middle Jurassic – Early Cretaceous rifting of the Danish
966 Central Graben. *Geological Survey of Denmark and Greenland Bulletin, 1*, 247 – 264.

967
968 Nagy et al., Finstad, E. K., Dypvik, H., & Bremer, G. A. (2001). Response of foraminiferal facies to
969 transgressive-regressive cycles in the Callovian of northeast Scotland. *Journal of foraminiferal*
970 *Research, 31*, 324 – 349.

971
972 National Infrastructure Commission (2018). *Cambridge, Milton Keynes and Oxford Future Planning*
973 *Options Project: Final Report (Revision A)* ([https://www.nic.org.uk/wp-content/uploads/NIC-](https://www.nic.org.uk/wp-content/uploads/NIC-FinalReport-February-2018-Rev-A-optimised.pdf)
974 [FinalReport-February-2018-Rev-A-optimised.pdf](https://www.nic.org.uk/wp-content/uploads/NIC-FinalReport-February-2018-Rev-A-optimised.pdf)).

975
976 Norris, S. (2017). Radioactive waste confinement: clays in natural and engineered barriers –
977 introduction. In Norris, S., Bruno, J., Van Geet, M., & Verhoef, E. (eds), *Radioactive Waste*
978 *Confinement: Clays in Natural and Engineered Barriers. Geological Society, London, Special*
Publications, 443, 1– 8.

979
980 Norris, M. A., & Hallam, A. (1995). Facies variations across the Middle – Upper Jurassic boundary in
981 Western Europe and relationship to sea level change. *Palaeogeography, Palaeoclimatology,*
982 *Palaeoecology, 116*, 189 – 245.

983
984 Norry, M. J., Dunham, A. C., & Hudson, J. D. (1994). Mineralogy and geochemistry of the
985 Peterborough Member, Oxford Clay Formation, Jurassic, UK: elemental fractionation during mudrock
986 sedimentation. *Journal of the Geological Society, London, 151*, 195 – 207.

987 Oksanen, J., Guillaume Blanchet, F., Friendly, M., Kindt, R., Legendre, P., McGlinn, D., Minchin, P.R.,
988 O'Hara, R.B., Simpson, G. L., Solymos, P., Stevens, M. H. H., Szoecs, E., & Wagner, H. (2018). vegan:
989 Community Ecology Package. R package version 2.5-2. <https://CRAN.R-project.org/package=vegan>.
990

991 Page, K. N., (2002). Brora (Callovian), Sutherland. In Cox, B. M., & Sumbler, M. G. (2002). *British*
992 *Middle Jurassic Stratigraphy. Geological Conservation Review Series No. 26, Joint Nature*
993 *Conservation Committee, Peterborough, 372 – 376.*
994

995 Page, K. N., Melendez, G., Hart, M. B., Price, G. D., Wright, J K., Bown, P., & Bello, J. (2009).
996 Integrated stratigraphical study of the candidate Oxfordian Global Stratotype Section and Point
997 (GSSP) at Redcliff Point, Weymouth, Dorset, UK. *Volumina Jurassica, 7, 101 – 111.*
998

999 Partington, M. A., Copestake, P., Mitchener, B. C., & Underhill, J. R. (1993). Biostratigraphic
1000 calibration of genetic stratigraphic sequences in the Jurassic – lowermost Cretaceous Hettangian to
1001 Ryazanian of the North Sea and adjacent areas. In Parker J. R. (Ed.), *Petroleum Geology of Northwest*
1002 *Europe: Proceedings of the 4th Conference, Geological Society, London* (pp. 371 – 386).
1003

1004 Pearce, C. R., Coe, A. L. & Cohen, A. S. (2010). Seawater redox variations during the deposition of the
1005 Kimmeridge Clay Formation, United Kingdom (Upper Jurassic): Evidence from molybdenum isotopes
1006 and trace metal ratios. *Paleoceanography, 25, PA4213.*
1007

1008 Penn, I. E., Cox, B. M. & Gallois, R. W. (1986). Towards precision in stratigraphy: geophysical log
1009 correlation of Upper Jurassic (including Callovian) strata of the Eastern England Shelf. *Journal of the*
1010 *Geological Society, London, 143, 381 – 410.*
1011

1012 Pharaoh, T. C., Morris, J. H., Long, C. B., & Ryan, P. D. (1996). *Tectonic Map of Britain, Ireland and*
1013 *adjacent areas, Sheet 1, 1:1 500 000.* Keyworth, Nottingham: British Geological Survey.
1014

1015 Powell, J. H., Rawson, P. F., Riding, J. B., & Ford, J. R. (2018). Sedimentology and stratigraphy of the
1016 Kellaways Sand Member (Lower Callovian), Burythorpe, North Yorkshire, UK. *Proceedings of the*
1017 *Yorkshire Geological Society, 62, 36 – 49.*
1018

1019 R Core Team (2020). *R: A language and environment for statistical computing.* Vienna, Austria: R
1020 Foundation for Statistical Computing. <https://www.R-project.org/>.
1021

1022 Rhys, G. H., Lott, G. K., Calver, M. A. (1981). The Winterborne Kingston borehole, Dorset, England.
1023 *Report of the Institute of Geological Sciences, 81/03.*
1024

1025 Robertson, A. H. F., & Ogg, J. G. (1986). Palaeoceanographic setting of the Callovian North Atlantic. In
1026 Summerhayes, C. P., & Shackleton, N. J. (Eds.), North Atlantic Palaeoceanography. *Special Publication*
1027 *of the Geological Society, London, 21, 283 – 298.*
1028

1029 Scheiber, J., Southard, J., & Thaisen, K. (2007). Accretion of Mudstone Beds from Migrating Floccule
1030 Ripples. *Science, 318, 1760 – 1763.*
1031

1032 Shephard-Thorn, E. R., Moorlock, B. S. P., Cox, B. M., Allsop, J. M., & Wood, C. J. (1994). Geology of
1033 the country around Leighton Buzzard. *Memoir of the British Geological Survey, Sheet 220* (England &
1034 Wales).

1035
1036 Smith, I F., & Edwards, J. W. F. (compilers). (1997). *Colour Shaded Relief Gravity Anomaly Map of*
1037 *Britain, Ireland and adjacent areas, 1:1500 0000 scale*. Keyworth, Nottingham, UK: British Geological
1038 Survey.
1039
1040 Soua, M. (2014). A Review of Jurassic Oceanic Anoxic Events as Recorded in the Northern Margin of
1041 Africa, Tunisia. *Journal of Geosciences and Geomatics, 2*, 94 – 106.
1042
1043 Southwood, T. R. E., & Henderson, P. A. (2000). *Ecological Methods*. Blackwell Science.
1044
1045 Taylor, S. P., Sellwood, B. W., Gallois, R. W., & Chambers, M. H. (2001). A sequence stratigraphy of
1046 the Kimmeridgian and Bolonian stages (late Jurassic): Wessex – Weald Basin, southern England.
1047 *Journal of the Geological Society, London, 158*, 179 – 192.
1048
1049 Thomas, R. D. K. (1978). Shell form and ecological range of living and extinct Arcoida. *Paleobiology*,
1050 *4*, 181 – 194.
1051
1052 Underhill, J. R. (1998). Chapter 8: Jurassic. In Glennie, K. W. (Ed.), *Petroleum Geology of the North*
1053 *Sea – Basic concepts and recent advances* (4th Edition). Blackwell Science.
1054
1055 Underhill, J. R., & Partington, M. A. (1993). Jurassic thermal doming and deflation in the North Sea:
1056 implications of the sequence stratigraphy evidence. *Geological Society, London, Petroleum Geology*
1057 *Conference Series 4*, 337 – 345.
1058
1059 Vavrek, M. J. (2016). A comparison of clustering methods for biogeography with fossil
1060 datasets. *PeerJ, 4*, e1720.
1061
1062 Weedon, G. P., Coe, A. L., & Gallois, R. (2004). Cyclostratigraphy, orbital tuning and inferred
1063 productivity for the type Kimmeridge Clay (Late Jurassic), Southern England. *Journal of the*
1064 *Geological Society, London, 161*, 655 – 666.
1065
1066 Whittaker, A., (Ed.). (1985). *Atlas of Onshore Sedimentary Basins in England and Wales: Post-*
1067 *Carboniferous Tectonics and Stratigraphy*. Glasgow: Blackie.
1068
1069 Whittaker, A., Holliday, D. W., & Penn, I. E. (1985). Geophysical logs in British Stratigraphy.
1070 *Geological Society Special Report, 18*, 74 pp.
1071
1072 Wignall, P. B. (1991). Test of the concepts of sequence stratigraphy in the Kimmeridgian (Late
1073 Jurassic) of England and northern France. *Marine and Petroleum Geology, 8*, 430 – 441.
1074
1075 Wignall, P. B. (1989). Sedimentary dynamics of the Kimmeridge Clay: tempests and earthquakes.
1076 *Journal of the Geological Society, London, 146*, 273 – 284.
1077
1078 Wignall, P. B., & Newton, R. (2001). Black shales on the basin margin: a model based on examples
1079 from the Upper Jurassic of the Boulonnais, northern France. *Sedimentary Geology, 114*, 335 – 356.
1080
1081 Wilby, P. R., Duff, K., Page, K. & Martin, S. (2008). Preserving the unpreservable: a lost world
1082 rediscovered at Christian Malford, UK. *Geology Today, 24*, 95 – 98.

1083

1084 Wilhelm, C. (2014). Notes on Maps of the Callovian and Tithonian Palaeogeography of the Caribbean
1085 Atlantic, and Tethyan Realms: Facies and Environments. *Geological Society of America Digital Map
1086 and Chart Series, 17*, 1 – 9.

1087

1088 Xu, W., Ruhl, M., Hesselbo, S. P., Riding, J. B., & Jenkyns, H. C. (2017). Orbital pacing of the Early
1089 Jurassic carbon cycle, black shale formation and seabed methane seepage. *Sedimentology, 64*, 127 –
1090 149.

1091

1092 **FIGURE CAPTIONS:**

1093

1094 Fig. 1. UK (Mid Callovian, E. coronatum Zone) palaeogeography for the Oxford Clay Formation, and
1095 location of key outcrop and borehole data referred to in this study. Palaeogeography based on
1096 Bradshaw et al. (1992, Map J8). Lines 1 & 2 are borehole correlation lines shown in Fig. 3. Map
1097 references for localities are given in text and/or *Supplementary Data*.

1098

1099 Fig. 2. The stratigraphy of the Oxford Clay Formation and coeval geological units in the Southern
1100 North Sea and Moray basins. Grey highlight indicates stratigraphy that is the focus of this study.
1101 Boreholes are continuously cored successions drilled for BGS, or partially cored successions drilled
1102 by others for hydrocarbons exploration (Ashdown 2, Kimmeridge 2) and held in the BGS national
1103 borehole archive at Keyworth, Nottingham. Biozonal nomenclature used in the text follows the
1104 conventions discussed by Cox (1990), in regarding Jurassic ammonite zones as chronostratigraphical
1105 units, referred to by species name with an initial capital letter written in non-italicized text. For
1106 clarity, we include the genus name on Figure 2, abbreviated by an initial letter for Subzones where
1107 this is the same as the genus used for the corresponding zone.

1108

1109 Fig. 3. Modelled thickness and correlation of the Peterborough Member. (A) Gamma ray log
1110 correlation: Southern North Sea - East Midlands Shelf - Wessex Basin - Channel Basin (Line 1 of Fig.
1111 1). (B) Gamma ray log correlation: East Midlands Shelf - Anglo-Brabant Massif - Weald Basin (Line 2
1112 of Fig. 1). (C) Interpolated thickness map showing faults (from Pharaoh et al. 1996) and borehole
1113 locations. Borehole numbering follows that used on Fig. 1. WWB (West Walton Beds); MD
1114 (measured depth, metres); TVD (true vertical depth, metres); gAPI (gamma ray American Petroleum
1115 Institute units). Cored boreholes (annotated) provide stratigraphical control for interpretations.

1116 Fig. 4. Gamma log correlation of the Oxford Clay Formation and Peterborough Member in the Weald
1117 and Wessex basins. Log interpretations are guided by the records from cored and geophysically
1118 logged boreholes, published log interpretations (e.g. Winterborne Kingston; Rhys et al., 1981), and
1119 related borehole data held in BGS data archives.

1120

1121 Fig. 5. Stratigraphy, geochemistry and biofacies of the CM9 and CM11 boreholes. Geochemical data
1122 show patterns of enrichment in shell (red curve) and detrital material (blue curve). The
1123 stratigraphical distribution of samples and their biofacies assignment is represented by the pattern
1124 of short horizontal lines plotted for each defined biofacies cluster (Chm 1, 2 etc). The composition of
1125 biofacies clusters is given in bar charts showing relative proportions of the key components,
1126 calculated by dividing the total number of records for each component by the total number of
1127 samples. See Supplementary Data for full details. Contrasting detail of shell beds at different levels in

1128 the succession are shown as core images for interval 'X' (sharp-based shell bed) and for interval 'Y'
1129 (shell bed with gradational base). 'C' and S1 – S15 are geochemical peaks discussed in the text.

1130

1131 Fig. 6. Lithology and biofacies of cored borehole successions in the Peterborough Member. Biofacies
1132 clusters are unique to each site and based on NERC clustering. See caption to Fig. 5 for explanation.
1133 NB: for clarity of other detail, shell hash not annotated on Eriswell log, but it is common throughout.
1134 * denotes lithologically and faunally distinct interval in Down Ampney 2 Borehole characterised by
1135 concentration of wood, foraminifera and bone.

1136 Fig. 7. Correlation and biofacies classification of Peterborough Member successions according to
1137 Duff (1974, 1975) compared with biofacies classifications assigned using DCA and NERC clustering.
1138 The comparison shows broad similarity in the pattern of classification deduced by the contrasting
1139 methodologies. The stratigraphical ranges of NERC biofacies clusters (Ca1, BL1, St1, NC1, etc.)
1140 corresponds with quantitative data for individual beds within each succession. The composition of
1141 biofacies clusters is given in bar charts showing percentages of key components in each NERC
1142 cluster.

1143 Fig. 8. Detrended Correspondence Analysis (DCA) of fossil assemblages in the Christian Malford CM
1144 11 (A) and Warlingham (B) boreholes, showing positions of samples and upper quartile taxa. The
1145 highly contrasting geometry of sample points with respect to key taxa at Warlingham compared to
1146 Christian Malford suggests a significantly contrasting relationship in the association of different taxa
1147 that characterise biofacies at the two sites. The distributions at Warlingham are inferred to be a
1148 mixing signal rather than an indication of altered palaeoecological relationships between taxa (see
1149 text for details). The proximity of Bositra and nuculacean bivalves on the DCA plot for Warlingham is
1150 reflected in their unusually close association in biofacies clusters throughout this succession (Fig. 7).
1151 See Fig. 7 for key to biofacies components. DCA plots for all cored boreholes forming part of this
1152 study are given in Supplementary Data.

1153 Fig. 9. Detrended Correspondence Analysis (DCA) for localities described by Duff (1974, 1975)
1154 showing positions of samples and upper quartile taxa, with samples classified according to NERC
1155 cluster assignment. See Fig. 7 for key to taxa. DCA plots for all cored boreholes forming part of this
1156 study are given in Supplementary Data.

1157 Fig. 10. Biozonal correlation of cored boreholes and key outcrops in the Peterborough Member.
1158 Borehole numbering follows that used on Fig. 1. Zn (Zone), Sz (Subzone), Gr (Grossouvrei), Ob
1159 (Obductum).

1160

1161 Fig. 11. Conceptual basin model for deposition of the Peterborough Member, showing key
1162 palaeogeographical and structural elements. 1: deltaic deposition in collapsed graben along crest of
1163 Mid-North Sea High; 2: thin successions with organic-rich mudstone on East Midlands Shelf; 3: highly
1164 condensed deposition with abundant shell hash on flanks of Anglo-Brabant Massif; 4: shell-rich
1165 mudstone at faulted margin of Weald Basin, fed by sediment from higher on flank of Anglo-Brabant
1166 Massif; 5: sediment-starved basin with thin, organic-rich and pyritic mudstone and limestone; 6:
1167 intra-basinal high with silty and sand-rich mudstone; 7: main depocentre underlain by extensive
1168 network of east-west faults, fed by sediment from flanks of Mid-North Sea High, East Midlands Shelf
1169 and pathways associated with the buried Worcester Graben. Note: vertical scale exaggerated.

1170 Fig. 12. The Worcester Graben defined by regional gravity data, with significant thickening of
1171 Peterborough Member occurring to the south and south-west, in line with the mouth of this

1172 structure. Black arrows denote likely sediment pathways. Gravity data from Smith and Edwards
1173 (1997), <https://www.bgs.ac.uk/datasets/gb-land-gravity-survey/>.

1174

1175 **Appendix 1 – Biofacies components and their abbreviation used in statistical analysis. Data list has**
1176 **been conditioned to remove species-level data (mainly applicable to data originally collected by**
1177 **Duff (1974, 1975))**

1178

1179	ammonite	(AM)
1180	ammonite spat	(AmS)
1181	<i>Anisocardia</i>	(Aic)
1182	aptychus	(AP)
1183	arcid	(AR)
1184	<i>Bathrotomaria</i>	(BA)
1185	belemnite	(BL)
1186	Belemnitheutis	(BT)
1187	bone	(BN)
1188	<i>Bositra</i>	(BO)
1189	bryozoan	(BR)
1190	burrowing	(BU)
1191	<i>Camptonectes</i>	(Ca)
1192	<i>Chlamys</i>	(CH)
1193	cirripede	(CI)
1194	coprolite	(CO)
1195	<i>Corbicella</i>	(CL)
1196	<i>Corbulomima</i>	(C)
1197	crinoid ossicle	(Cr)
1198	<i>Dicroloma</i>	(DI)
1199	<i>Discomiltha</i>	(Dm)
1200	Echinoid spine	(Es)
1201	<i>Entolium</i>	(EN)
1202	foraminifera	(FO)
1203	gastropod (juvenile)	(GJ)

1204	<i>Genicularia</i>	(GE)
1205	<i>Grammatodon</i>	(GR)
1206	<i>Gryphaea</i>	(GY)
1207	Shell hash	(HS)
1208	Hooks (belemnoid)	(HO)
1209	<i>Isocyprina</i>	(IS)
1210	<i>Isognomon</i>	(IG)
1211	<i>Lingula</i>	(Li)
1212	<i>Mastigophora</i>	(MA)
1213	<i>Mecochirus</i>	(MS)
1214	<i>Meleagrinella</i>	(ME)
1215	<i>Mesosacella</i>	(MC)
1216	<i>Modiolus</i>	(MO)
1217	<i>Myophorella</i>	(MP)
1218	<i>Nanogyra</i>	(NG)
1219	<i>Neocrassina</i>	(NE)
1220	<i>Nicaniella</i>	(NI)
1221	nuculaceans	(NU)
1222	<i>Ooliticia</i>	(OO)
1223	Ophiuroid	(OP)
1224	<i>Orbiculoidea</i>	(Orb)
1225	ostracod	(OS)
1226	otolith	(OT)
1227	<i>Oxytoma</i>	(OX)
1228	oyster	(OR)
1229	<i>Parainoceramus</i>	(PA)
1230	<i>Pecten</i>	(PN)
1231	<i>Pholadomya</i>	(PM)
1232	<i>Pinna</i>	(PIN)
1233	<i>Plagiostoma</i>	(PG)
1234	<i>Pleuromya</i>	(PL)

1235	<i>?Praecoria</i>	(PRa)
1236	<i>Procerithium</i>	(PR)
1237	<i>Protocardia</i>	(PC)
1238	<i>Pteroperna</i>	(PT)
1239	<i>Quenstedtia</i>	(QU)
1240	rhynchonellid	(Rh)
1241	<i>Rollierella</i>	(Ro)
1242	scaphopod	(SC)
1243	serpulid	(SE)
1244	shell hash	(HS)
1245	<i>Solemya</i>	(SO)
1246	solitary coral	(Sco)
1247	spat	(SP)
1248	sponges	(Spo)
1249	terebratulid	(TE)
1250	<i>Thracia</i>	(TH)
1251	trigoniid	(Tr)
1252	wood	(W)

1253

1254 **Appendix 2 – Other abbreviations used in statistical outputs**

1255	Athleta Zone	(Az)
1256	Calloviense Subzone	(Csz)
1257	Calloviense Zone	(Caz)
1258	Combined Coronatum,	
1259	Jason, Calloviense	
1260	Zones	(CJC)
1261	Coronatum Zone	(Cz)
1262	Enodatum Subzone	(Esz)
1263	Grossouvrei Subzone	(Gsz)
1264	Jason Subzone	(JsZ)
1265	Jason Zone	(Jz)

1266 Medea Subzone (Msz)

1267 Phaeinum Subzone (Psz)

1268 Sample Size (Sz)

1269